

Kaunas University of Technology
Faculty of Mechanical Engineering and Design

Design of Experimental Setup for Measuring Electrical Conductivity of Titanium Composite Samples

Master's Final Degree Project

Donatas Gričius

Project author

Assoc. prof. Rasa Kandrotaitė Janutienė

Supervisor

Kaunas, 2022



Kaunas University of Technology
Faculty of Mechanical Engineering and Design

Design of Experimental Setup for Measuring Electrical Conductivity of Titanium Composite Samples

Master's Final Degree Project
Mechatronics (6211EX017)

Donatas Gricius

Project author

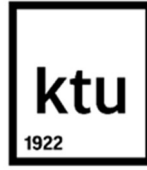
**Assoc. prof. Rasa Kandrotaitė
Janutienė**

Supervisor

Lect. Darius Mažeika

Reviewer

Kaunas, 2022



Kaunas University of Technology
Faculty of Mechanical Engineering and Design
Donatas Gricius

Design of Experimental Setup for Measuring Electrical Conductivity of Titanium Composite Samples

Declaration of Academic Integrity

I confirm the following:

1. I have prepared the final degree project independently and honestly without any violations of the copyrights or other rights of others, following the provisions of the Law on Copyrights and Related Rights of the Republic of Lithuania, the Regulations on the Management and Transfer of Intellectual Property of Kaunas University of Technology (hereinafter – University) and the ethical requirements stipulated by the Code of Academic Ethics of the University;
2. All the data and research results provided in the final degree project are correct and obtained legally; none of the parts of this project are plagiarised from any printed or electronic sources; all the quotations and references provided in the text of the final degree project are indicated in the list of references;
3. I have not paid anyone any monetary funds for the final degree project or the parts thereof unless required by the law;
4. I understand that in the case of any discovery of the fact of dishonesty or violation of any rights of others, the academic penalties will be imposed on me under the procedure applied at the University; I will be expelled from the University and my final degree project can be submitted to the Office of the Ombudsperson for Academic Ethics and Procedures in the examination of a possible violation of academic ethics.

Donatas Gricius

Confirmed electronically



Kaunas University of Technology
Faculty of Mechanical Engineering and Design

Task of the Master's final degree project

Given to the student – Donatas Gričius

1. Title of the project

Design of Experimental Setup for Measuring Electrical Conductivity of Titanium Composite Samples

(In English)

Titano kompozito bandinių elektrinio laidumo matavimo stendo kūrimas

(In Lithuanian)

2. Hypothesis:

The metal matrix composite has a lower electrical conductivity than the electrical conductivity of its constituent materials.

3. Aim and tasks of the project

Aim: To develop and test an experimental setup for measuring electrical conductivity of Titanium metal matrix composites.

Tasks:

1. To design and perform simulation of an electrical conductivity measurement setup.
2. To fabricate an electrical conductivity measurement setup.
3. To measure electrical conductivity of Titanium metal matrix composites and analyse results.
4. To perform cost analysis of measurement setup.

4. Initial data of the project

Measurement setup must be able to measure resistivity in the range of $10^{-6} \Omega\text{m}$.

5. Main requirements and conditions

Solidworks and COMSOL software, Titanium based composite samples, nanovoltmeter, current source, temperature sensor, copper sample.

Project author	Donatas Gričius	2022.02.28
	<i>(Name, Surname)</i>	<i>(Signature)</i> <i>(Date)</i>

Supervisor	Rasa Kandrotaitė Janutienė	2022.02.28
	<i>(Name, Surname)</i>	<i>(Signature)</i> <i>(Date)</i>

Head of study field programs	Regita Bendikienė	2022.02.28
	<i>(Name, Surname)</i>	<i>(Signature)</i> <i>(Date)</i>

Gricius, Donatas. Design of Experimental Setup for Measuring Electrical Conductivity of Titanium Composite Samples. Master's Final Degree Project, supervisor Assoc. prof. Rasa Kandrotaitė Janutienė; Faculty of Mechanical Engineering and Design, Kaunas University of Technology.

Study field and area (study field group): Production and Manufacturing Engineering (E10), Engineering Sciences (E).

Keywords: Electrical conductivity, resistivity, four probe, Titanium metal matrix composite, measurement setup.

Kaunas, 2022. 60 p.

Summary

An electrical conductivity measurement tool is needed for characterization of Titanium based composite samples. The powder-based metal matrix composite samples are novel, fabricated by using high voltage electric discharge and spark plasma sintering processes. They have potential usage in the aviation industry. The composite samples are small and have a pellet shape. Other research that measured electrical conductivity of Titanium based composites was reviewed. A collinear four-point probe method was chosen for measurement of electrical conductivity. Needle like test probes were used to contact the tested sample. Other aspects of the measurement setup are discussed and selected according to relevant literature. A simulation was performed using COMSOL software to validate the measurement method. Furthermore, a simulation performed for contact force of the probes was performed. A 3D model of the measurement tool was created and designed. It was chosen to implement a sample holder and a probe holder for fixing the sample and test probes. The needle holder has the function to rotate. A linear drive is used to move the sample into the test probes. A Peltier element is used to heat or cool the sample. A temperature sensor is used to monitor the temperature of the Peltier element. The full width of the measurement tool is 120 mm, length – 228 mm and height – 323 mm. The measurement setup is controlled with Arduino board. An electrical schematic was presented, connections and components were explained. The measurement setup was fabricated using various operations, such as milling, turning, drilling. The measurement setup was tested and validated by using a copper sample. Six Titanium composite samples electrical resistance was measured, and electrical conductivity calculated. Furthermore, samples were measured at different temperatures and resistivity dependence to temperature was presented. Experimental results are compared to similar research results. Measurement setup was evaluated from economical point of view and cost analysis was performed.

Gricius, Donatas. Titano kompozito bandinių elektrinio laidumo matavimo stendo kūrimas. Magistro baigiamasis projektas, vadovė doc. Rasa Kandrotaitė Janutienė; Kauno technologijos universitetas, Mechanikos inžinerijos ir dizaino fakultetas.

Studijų kryptis ir sritis (studijų krypčių grupė): Gamybos inžinerija (E10), Inžinerijos mokslai (E).

Reikšminiai žodžiai: Elektrinis laidumas, specifinė varža, Titano metalo matricos kompozitas, matavimo stendas, keturių taškų matavimas.

Kaunas, 2022. 60. p.

Santrauka

Elektrinio laidumo stendas reikalingas, kad charakterizuoti titano pagrindo sukurtus kompozitus. Miltelių pagrindu sukurti metalo matricos kompozitai yra nauja medžiaga pagaminta naudojant aukštos įtampos elektros iškrovos ir kibirkštinio plazmos sukepinimo procesus. Šie kompozitai turi potencialo būti naudojami aviacijoje. Kompozito bandiniai yra maži ir turi granulės formą. Atliekama kitų tyrimų apžvalga, kurie matavo titano pagrindo kompozitus. Pasirinktas keturių taškų matavimo metodas, kai matavimo kontaktai išdėstyti vienoje linijoje. Adatėlių tipo matavimo kontaktai naudojami kontaktuoti bandiniui. Kiti matavimo stendo aspektai yra apžvelgiami ir tinkamiausias variantas pasirenkamas atsižvelgiant į literatūrą. Atliekama simuliacija naudojant COMSOL programinę įrangą, kad validuoti matavimo metodą. Simuliacija dar atliekama kontakto jėgai charakterizuoti. Matavimo įrangos 3D modelis yra sukuriamas ir suprojektuojamas. Pasirenkama naudoti bandinio ir adatėlių laikiklius, kad juos pritvirtinti. Adatėlių laikiklius gali sukurti apie savo ašį. Linijinė pavara naudojama pakelti ir nuleisti bandinį. Peltier elementas naudojamas bandiniui pakaitinti ir šaldyti. Temperatūros jutiklis naudojamas stebėti Peltier elemento temperatūrai. Pilna stendo geometrija yra 120 mm plotis, 228 mm ilgis ir 323 mm aukštis. Linijinė pavara ir kiti elementai yra kontroliuojami su Arduino moduliu. Pateikiama elektrinė schema, jungimas ir elementai yra paaiškinami. Matavimo stendas yra pagaminamas naudojant įvairias apdirbimo operacijas, tokias kaip tekinimas, frezavimas, gręžimas. Matavimo stendas ištestuojamas ir validuojamas naudojant vario bandinį. Šešių titano kompozito bandinių varža išmatuojama ir apskaičiuojamas elektrinis laidumas. Titano bandiniai dar išmatuojami prie skirtingų temperatūrų, gaunama specifinės varžos ir temperatūros priklausomybė. Duomenys gauti eksperimentiniu būdu yra palyginami su rezultatais gautais kituose panašiuose tyrimuose. Matavimo stendas yra apžvelgiamas iš ekonominės pusės ir jam atliekama kaštų analizė.

Table of contents

List of figures	8
List of tables	9
List of abbreviations.....	10
Introduction	11
1. Literature review of composites electrical conductivity measurement	12
1.1. Relevance and novelty of Titanium composites and their electrical conductivity measurement 12	
1.2. Review of Titanium based metal matrix composites electrical conductivity research	16
1.3. Review of electrical conductivity measurement designs.....	19
2. Methodology for selecting electrical conductivity measurement principle.....	21
2.1. Selection of electrical conductivity measurement method.....	21
2.2. Electrical conductivity measurement environment conditions.....	22
2.3. Current source and voltage measurement selection	23
2.4. Simulation of colinear four-point probe measurement.....	23
2.5. Simulation of probes contact force to sample	25
3. Development of electrical conductivity measurement setup	27
3.1. Modeling of electrical conductivity measurement setup.....	27
3.2. Fabrication of electrical conductivity measurement setup	30
3.3. Control and electrical part of electrical conductivity measurement setup.....	34
4. Testing electrical conductivity of Titanium metal matrix composite samples.....	37
4.1. Discussion of measurement results	41
5. Cost analysis of fabricating electrical conductivity measurement setup.....	43
Conclusions	45
List of references.....	46
Appendices	49

List of figures

Fig. 1. TiC with 20 wt% Ti3Al composite microstructure with aluminium mapping sintered at 1500 °C [10]	12
Fig. 2. Spark plasma sintering (SPS) working principle [12]	13
Fig. 3. Lightning dissipation in airplane [16].....	14
Fig. 4. Sample connection according to Van der Pauw method [18].....	15
Fig. 5. Electrical resistivity at different annealing temperatures [11].....	16
Fig. 6. Collinear four-point probe method [11].....	17
Fig. 7. Electrical conductivity dependence on vol% Al ₂ O ₃ [4].....	18
Fig. 8. Collinear four point probe design for resistivity measurement [21].....	19
Fig. 9. Apparatus for measuring surface resistance and resistivity at high temperature [22]	19
Fig. 10. Apparatus for resistivity measurement in high-temperature range [23]	20
Fig. 11. Current path of semi-infinite 3D material [7]	22
Fig. 12. Sample and probe arrangement model in COMSOL.....	24
Fig. 13. Electric potential plot of collinear for point probe method from COMSOL	24
Fig. 14. von Mises stress plot with 8 N force applied.....	26
Fig. 15. Model of sample holder	27
Fig. 16. Model of cooling element	28
Fig. 17. Model of needle holder	28
Fig. 18. Electrical conductivity measurement setup Solidworks model: 1 – Sample; 2 – Sample holder; 3 – Peltier element; 4 – Test needles; 5 – Needle holder; 6 – Fixing element; 7 – Linear guides; 8 – Bracket; 9 – Linear motion drive; 10 – Cooling element; 11 – Top housing; 12 – Housing rod; 13 – Bottom housing.	29
Fig. 19. Electrical conductivity measurement setup cross section view: 1 – Sample; 2 – Sample holder; 3 – Peltier element; 4 – Test needles; 5 – Needle holder; 6 – Fixing element; 7 – Linear guides; 8 – Bracket; 9 – Linear motion drive; 10 – Cooling element; 11 – Top housing; 12 – Housing rod; 13 – ISO 7045 M3 x 10 bolt; 14 – ISO 7380 M5 x 12 bolt; 15 – ISO 4762 M3 x 25 bolt; 16 – ISO 7045 M3 x 30 bolt; 17 – ISO 4034 M6 nut; 18 – ISO 4762 M6 x 35 bolt.....	30
Fig. 20. Fabricated sample holder	31
Fig. 21. Needle holder, a) after turning; b) finished part.....	32
Fig. 22. Cooling element, a) after cutting; b) finished part.....	32
Fig. 23. Top housing with linear guides.....	33
Fig. 24. Fully assembled measurement setup.....	34
Fig. 25. Circuit of electrical part: 1 – 12V power supply; 2 – L298N motor driver; 3 – Arduino Uno; 4 – DS18B20 digital temperature sensor; 5 – LCD screen; 6 – Potentiometer; 7 – Linear drive.	35
Fig. 26. Schematic of electrical part.....	36
Fig. 27. Test needles contacting the sample.....	37
Fig. 28. Keithley 2614B source meter.....	37
Fig. 29. Samples electrical resistivity dependence on temperature.....	41
Fig. 30. Ossila Four-Point Probe System [30]	44

List of tables

Table 1. Comparison of Ti-Al-C composites properties.....	18
Table 2. Geometrical parameters of samples.....	21
Table 3. Contact force simulation results	26
Table 4. Sample holder fabrication process.....	30
Table 5. Needle holder fabrication process.....	31
Table 6. Cooling element fabrication process	32
Table 7. Top housing fabrication process	33
Table 8. Bottom housing fabrication process	34
Table 9. Ti composite samples electrical resistance measurement results	38
Table 10. Average electrical resistance measurement results.....	39
Table 11. Average electrical resistance measurement results after current reversal method	39
Table 12. Samples electrical resistivity and conductivity.....	40
Table 13. Samples resistance measurement results at different temperatures.....	40
Table 14. Ti composite samples composition and fabrication parameters	42
Table 15. Comparison of electrical resistivity obtained by different ways	42
Table 16. Cost of material for electrical conductivity measurement setup	43
Table 17. Labor cost of fabricating measurement setup	44

List of abbreviations

Abbreviations:

MMC – metal matrix composite.

HVED – high-voltage electric discharge.

SPS – spark plasma sintering.

Ti – Titanium.

SOFC - Solid oxide fuel cells.

EMI - electromagnetic interference.

SLM - selective laser melting.

DC – direct current.

AC – alternate current.

LCD – liquid crystal display.

Introduction

Ti based metal matrix composites are novel materials that have superior mechanical properties. These composites have potential to be used in the aviation industry for their good specific strength, lightweight, heat and wear resistance [1]. They are already used in aircraft engines and gas turbines [1, 2]. Material properties of these novel composites must be studied and tested. One of the important properties is electrical conductivity. To measure electrical conductivity, a measurement setup suitable for composite samples is needed.

Like metals, Ti composites are good electrical conductors. They have an electrical conductivity in the range of 10^6 S/m [3, 4]. The electrical conductivity of a composite depends on many factors, such as: chemical composition, particle size, porosity, homogeneity, isotropy, manufacturing method. The Ti-Al composites are manufactured using high voltage electric discharge (HVED) and spark plasma sintering (SPS) methods from powders. After HVED process composite contains carbides and MAX phases. Also, the particle size is reduced and all components are distributed evenly [2]. Porosity inside the microstructure occurs due to air bubbles that appear during manufacturing and interaction between matrix and reinforcement particles [5]. The optimal ratio between the constituent components at which both electrical and mechanical properties are optimal is important to find. Most powder based metal matrix composites are isotropic in nature [6]. Four point probe method is commonly used to measure electrical conductivity of such composite samples [3, 4]. When utilizing this method, the sample geometry must be considered, and appropriate corrections made. Ideally, test sample should have uniform geometry and thickness. Also, sample test surface should be polished to minimize surface roughness, pores and contaminants [4]. The probes must contact the sample with small point contacts and be spaced evenly. Probes are arranged in a straight line. Two outer probes have current running through them, and two inner probes are measuring potential difference. This method eliminates parasitic resistance coming from probe contact. The force of probes into sample should be constant and equal with all probes [7]. The electrical conductivity dependence on temperature is an important characteristic. Sample heaters or coolers are commonly used in measurement setups. It is known that electrical conductivity increases at lower temperature. Furthermore, measurements under controlled atmosphere for instance vacuum eliminates errors coming from humidity. The current source applied should be pulsed DC or AC to prevent Joule heating of the sample, which could influence the result. Voltage measurements must be conducted with sensitive nanovoltmeter. Outside interference that could affect measurement must be considered.

This work will advance knowledge about Ti metal matrix composites electrical conductivity properties. Improved ways for measuring electrical conductivity of metal matrix composites are proposed. Also, experimental data of electrical conductivity for bulk pellet shape samples of finite geometry is acquired. Research for such shape composite samples is limited. The influence of outside factors such as temperature and atmosphere are researched.

Aim: To design and test an experimental setup for measuring electrical conductivity of Titanium metal matrix composites.

Tasks:

1. To design and perform simulation of an electrical conductivity measurement setup.
2. To fabricate an electrical conductivity measurement setup.
3. To measure electrical conductivity of Titanium metal matrix composites and analyse results.
4. To perform cost analysis of measurement setup.

1. Literature review of composites electrical conductivity measurement

1.1. Relevance and novelty of Titanium composites and their electrical conductivity measurement

Metal matrix composites are novel materials with improved mechanical characteristics compared to regular alloy metals. Metal matrix composites are composed of at least two materials, one of which must be a metal. In this research Ti-Al based metal matrix composites was analyzed and tested. Titanium is a very advantageous material that is in high demand in many industries because of its combination of properties, such as corrosion resistance and high specific strength. However, titanium is relatively expensive because of its manufacturing processes [8]. Aluminum is cheap, widely available, also, it is a lightweight material. Titanium is usually used as the matrix and other materials are used as reinforcement. These types of composites are also called – titanium matrix composites or TMCs. Different reinforcement materials, their combinations and amounts can be used to create the desired property composites [8].

The main application area of Ti based composites is in the aviation industry. The aviation industry requires high strength and wear resistant materials that are lightweight. Titanium based composites fulfill this requirement having a good strength to weight ratio and are good candidates to replace steel and aluminum parts. These composites could be used for making airframes, fuselages, gas turbine engines, hydraulic tubes in airplanes, helicopters, and spacecrafts [2, 8]. The usage of these composites reduces the fuel consumption of aircrafts and in turn reduce CO₂ emissions and flight costs. Similarly, in the automotive industry, they can be used for body, exhaust valves, spring suspension. Also, it was found that Ti-Al based composites are suitable for car brake discs. These composites are lightweight, can withstand high temperatures and have high wear resistance [9]. Another big sector, where Ti based composites could be used is in biomedical industry. Titanium has good bio-compatibility and by using appropriate reinforcement materials, it could be used as bone or dental implants [8]. The main problem associated with metal matrix composites is their manufacturing methods.

In Fig. 1, a SEM image of the microstructure of TiC with 20 wt% Ti₃Al that was sintered at 1500 °C is shown. In the right image, a mapping of aluminium is shown, it is highlighted in white color. It can be seen that aluminium particle size is around 15 to 35 µm. In the left image open pores can also be seen. Titanium and carbon elements represent the black color in the image.

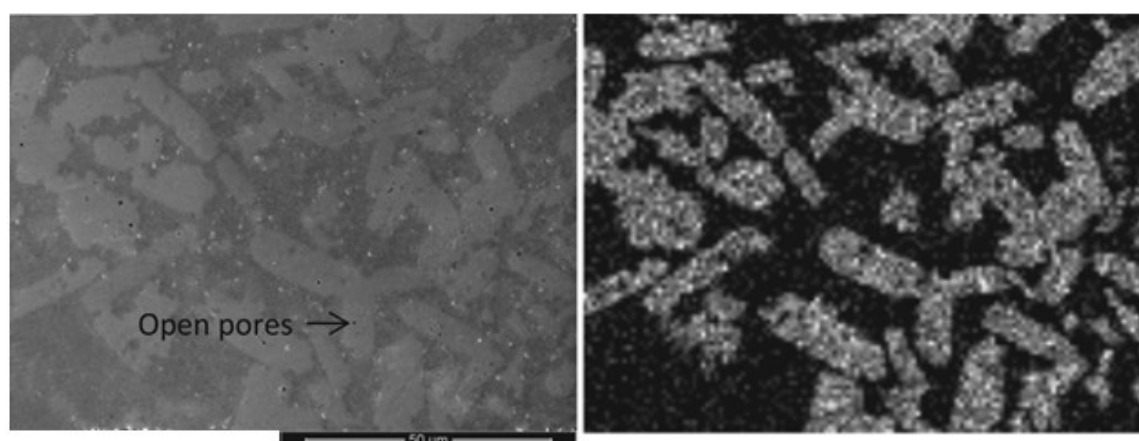


Fig. 1. TiC with 20 wt% Ti₃Al composite microstructure with aluminium mapping sintered at 1500 °C [10]

Another novel development in metal matrix composites is MAX phases. MAX phases are the combination of three materials, an early transition metal, an element from the A group periodic table and carbon or nitrogen. An example of MAX phase material would be Ti_2AlC composite. MAX phase material exhibit both metal and ceramic properties. They usually have good mechanical properties, hardness, electrical and thermal conductivities. This mix of properties can be attributed to the covalent, ionic, and metallic bonds in the structure. MAX phases have laminar hexagonal crystalline structure. These materials can be produced by hot pressing, spark plasma sintering, hot isostatic pressing and others. MAX phase materials have been a subject of heavy research in recent years [11].

A lot of research is made to find an optimal way to produce metal matrix composites [2, 8]. It is important for the matrix and reinforcement materials to have a strong bond with each other. Usually, metal matrix composites are created from fine powders. If the particle sizes are in the range of nm, they can be called nanocomposites. The particle size, porosity, homogeneity, isotropy influences the composite properties together with the manufacturing process. To achieve even particle distribution throughout the composite, ball milling is commonly used. To further improve the homogeneity and bond strength, some researchers use HVED. HVED is the process of applying pulsed electric discharges to particles while submerged into liquid. Later the particles are consolidated by SPS method [2]. In Fig. 2, the SPS method is shown, DC current pulses are running through two cylindrical punches/electrodes. In-between the punches, there are graphite dies, which form the powders into pellets. Additive manufacturing is also heavily researched method in producing metal matrix composites. The selective laser melting (SLM) method is commonly used [8].

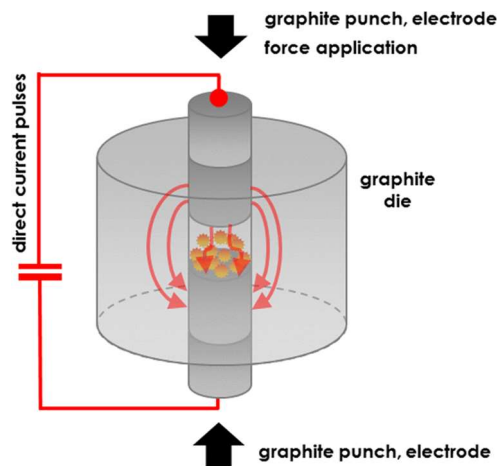


Fig. 2. Spark plasma sintering (SPS) working principle [12]

There is a need to find and measure mechanical and electrical properties of such novel materials. Measurements and tests are performed after manufacturing to find optimal ratio of the matrix and reinforcement materials. Often the percolation zone or the point at which wanted parameters don't change anymore is searched. Electrical conductivity or resistivity is one of those important parameters. The current knowledge of Ti-Al composites electrical conductivity and its measurement methods is limited. In some Ti-Al composite applications, the electrical properties are not very important, but there are areas where knowing the electrical conductivity is very important. An example is shown with Al_2O_3/Ti ceramic composites. A hybrid ceramic/metal composite can achieve unique properties. They have potential for temperature sensitive devices, varistors, fuel cell electrodes. Also, it would allow to use electrical discharge machining for ceramic materials [13]. It also has been demonstrated that TiC-Ti₃Al composites can be used for Solid Oxide Fuel Cells

(SOFC) used in vehicle applications. The SOFC interconnects must have high electrical conductivity, low contact resistance and high thermal conductivity [10]. Another application for aluminium metal matrix composites was found in electrical wires and electronics as a substitute to copper. In the study it was shown that Al, Ti and B composite has very good electrical conductivity [14].

An important aspect in the aviation industry is the quality control methods. A common non-destructive testing method is using Eddy currents. The material under test must be conductive when Eddy current technique is used [15]. Other aspects in the aviation industry are lightning strike protection and electromagnetic interference (EMI) shielding. Since aircrafts fly several kilometers in the sky, they are subjected to lightning strikes and electromagnetic fields created by the lightning. Both problems can be solved by using conductive materials. If a lightning strike hits a conductive material, it scatters over the whole body of the airplane and minimize the damage. On the other hand, if lightning hits an insulative material it does significant damage [16, 17]. Metal meshes are sometimes used on the outer side of the airplane for lightning protection [17]. In Fig. 3, a visualization of lightning strike dissipation is shown. Initial entry of the lightning into the aircraft is scattered over the body. The exit of the lightning is also shown in multiple areas. Lightning creates charge and electromagnetic fields on the airplane.

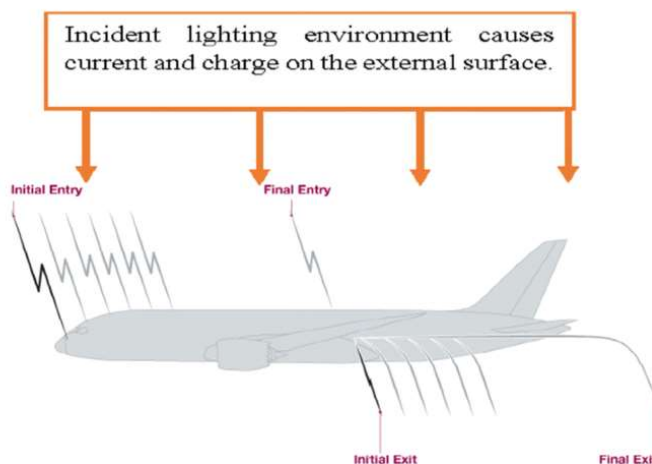


Fig. 3. Lightning dissipation in airplane [16]

With electromagnetic field shielding, a conductive material forms a Faraday cage and stops the electromagnetic fields. Electromagnetic field shielding is important for protecting sensitive electronics from malfunctioning in the aircraft. An innovative material with conductive, lightweight and high strength properties is being searched and developed to replace current non-conductive composites [16]. Another area where conductive materials in aviation is needed is; the deicing of airplane wings. This is more applicable on smaller planes without jet engines. On larger airplanes, exhaust heat from the engine is used for deicing. In certain designs removing ice by using electricity and Joule heating is preferable and for that an electrically conductive material is needed. Conductive composites are being developed for this application [17].

There are many methods and ways to measure electrical conductivity or resistivity. Generally, the measurement method chosen depends on the electrical conductivity of the measured material. In the case of this research, most Ti-Al composites fall in the range of $10^{-6} \Omega\text{m}$ [10]. It can be assumed that the tested samples will be in this range. Traditional electrical conductivity measurement utilizes two electrodes and measures resistance directly. Later by knowing the sample geometry, the resistivity or

conductivity can be calculated. The problem with this method; is that the electrodes introduce large contact resistance. The contact resistance is minimized when using a four-point probe method. In this method, electrode contact area to the sample is very small. Two probes are used to drive current through the sample and the remaining probes measure the voltage in the sample. The resistance is calculated by using Ohms law and the resistivity by using appropriate formulas. There are several configurations of the four-point probe method, when probes are distributed in one line and when the probes are distributed evenly on the sides, the latter is called Van der Pauw method. The colinear four-point probe method is more commonly used for thin samples and the Van der Pauw is more commonly used for bulk samples. In this research, circular samples were used. The Van der Pauw method requires the sample to have equal height throughout its geometry, be homogenous and isotropic. Most metal matrix composites made from powders are homogenous and isotropic. With this method measurement is repeated for four times at different spots on the sample. Also, measurements are performed at both polarities to offset thermoelectric effect. A modified version of the Van der Pauw can be used for measuring anisotropic samples, it is called the Montgomery method [7]. In Fig. 4, a Van der Pauw connection to sample can be seen. DUT, means a device under test, it represents the sample. The letters M, N, P, O represent the electrodes. The electrodes are electrically connected to the measurement circuit. Other parts are isolated from the circuit by insulative material – SiO₂ substrate. I_{MN} represents current flow between two electrodes and V_{PO} represents voltage measurement electrodes.

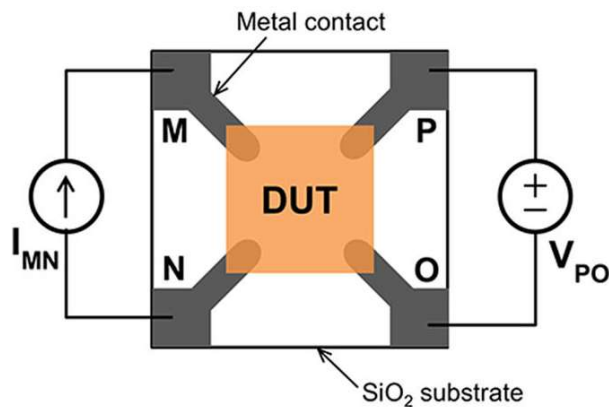


Fig. 4. Sample connection according to Van der Pauw method [18]

The difference between measuring regular materials and composites is the resistance appearing because of grain boundaries between particles. It has been shown that grain boundaries increase the resistance theoretically and experimentally [19]. The porosity that occurs in powder composites is another property that theoretically should increase resistance but has not been studied experimentally. The environment conditions such as temperature and atmospheric pressure are very important when trying to accurately determine material properties. Most of the found measurement setups consisted of large heating furnaces and vacuum tubes in which the sample is placed [18]. Set-ups with cooling chambers are even more complicated and big. The temperature dependence on resistivity of Ti-Al metal matrix composites is not fully known. Furthermore, the impact of Joule heating to the measurement result is not concise. The best current application method pulsed DC or AC is not tested. A simpler more compact measurement set up is needed that would also be suitable for composite materials.

1.2. Review of Titanium based metal matrix composites electrical conductivity research

Several similar research and their results were presented and analyzed. In the first article Ti-Al-C composites were produced by combining TiC and Ti₃Al powders. Ti₃Al powder varied from 10 to 40 wt%. The TiC powder used was synthesized from carbon coated titania and nano sized. Powders were mixed by using dry mixing in a bottle using two methacrylate balls for 1 hour. Pellets were made by using a uni-axial press under 50 MPa pressure in a hardened steel die that had a diameter of 12.95 mm. Pellets were solidified by using sintering without pressure in vacuum at 1100 °C to 1500 °C temperature for 1 hour. Electrical conductivity measurements were made under regular air, while sample was kept at 800 °C. Measurements are made 10 times every 10 hours, at different temperatures. Sample was a rectangle with 3×3×10 mm dimensions. A Kelvin 4 wire method was used on an AC resistance bridge. The results show that less percentage of Ti₃Al increases the electrical conductivity and more decreases. The increase in electrical conductivity is due to the formation of Al₂O₃ and higher porosity from Ti₃Al powder. Also, electrical conductivity decreased as holding time increased. At 10 wt% the initial measurement was 1200 S/cm and 270 S/cm with 40 wt% [10].

In the second study, thin film Ti₂AlC and Ti₃AlC₂ MAX phase composites were produced and tested. Magnetron sputtering is used to deposit Ti, Al and C layers 22 times each. The final thin film was 500 nm thick. Later thin film was annealed with rapid thermal processing in Argon and Hydrogen atmosphere under 650 °C to 1000 °C. The resistivity measurements were performed using Van der Pauw method in linear configuration. A Keithley 2400 current source was used to excite current between probes, 01 mA used. Two Keithley multimeters were used for measuring the resultant voltage and current. LabVIEW software was used to perform measurements and digital camera to measure position between probes. All probes had spring tips, so that equal pressure would be between all the probes. The results showed, that at lower temperatures 650 to 800 °C resistivity is higher than at higher temperatures. It can be attributed to grain size, grain boundaries and phase transition. After 850 °C, the resistivity starts to increase, most likely due to formation of Al₂O₃. The highest electrical resistivity was at 650 °C, approximately 10⁻⁶ Ωm and the lowest was at 850 °C, approximately 0.54·10⁻⁶ Ωm. In Fig. 5, the dependence of electrical conductivity and annealing temperature of the composite is shown. Electrical conductivity measurement performed every 50 °C. It can be seen that Ti₂AlC has phase change to Ti₃AlC₂ at 800 to 900 °C [11].

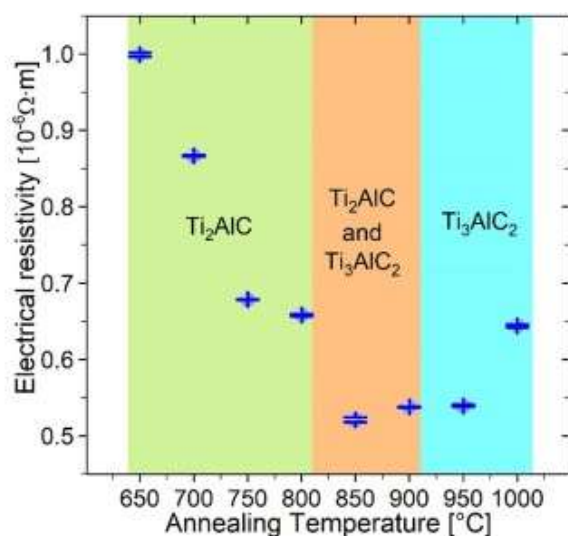


Fig. 5. Electrical resistivity at different annealing temperatures [11]

Another study compared bulk Ti-Al-C composite with the same coating material. The bulk sample was produced by sintering at 1350 °C for 30 min in vacuum atmosphere. Later it was hot-pressed at 1350 °C for 30 min in air and 30 MPa pressure. The sample was rectangular shape with 4×4×35 mm dimensions. The final composite composition was 95 wt% Ti₂AlC and 5 wt% TiC. Electrical conductivity was measured using the four-probe method under normal air atmosphere and 20 °C temperature. The spacing between probes was 1.4 mm. The research goal was to treat the composite to high temperature and see how oxidation affects the electrical conductivity. Electrical conductivity was measured after heating sample to 600 °C and keeping it at that temperature for 1000 hours. It was found that the bulk sample had significantly lower electrical conductivity compared with coating, it decreased very little. Initial measurement of bulk sample was $1.63 \cdot 10^6$ S/m and $1.33 \cdot 10^6$ S/m for coating respectively. After temperature treatment bulk sample electrical conductivity decreased to $1.73 \cdot 10^2$ S/m. The decrease in electrical conductivity can be explained by the formation of aluminum and titanium oxides at the sample surface at high temperatures [3]. In Fig. 6, an illustration of the linear four-point probe configurations. Two outer probes are driving current through the sample and the middle probes measure voltage.

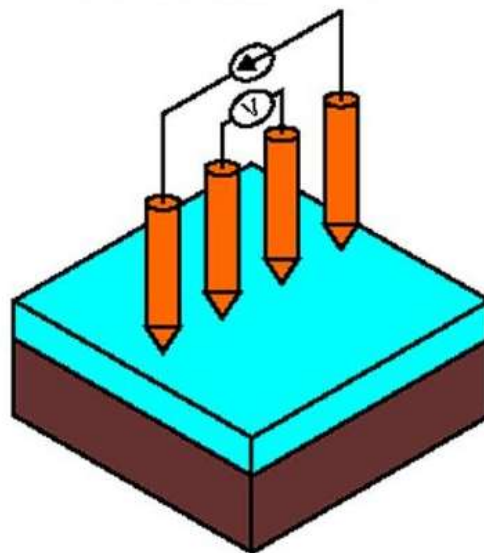


Fig. 6. Collinear four-point probe method [11]

A different study analyzed relationship between Ti₃AlC₂ and Al₂O₃ powder composite. Ratio of 5 to 25 vol% Al₂O₃ was mixed with Ti₃AlC₂ to create a new composite with better strength and hardness. All the powders were ball milled in ethanol for 24 hours. Later they were dried and formed in a graphite mold under 20 MPa pressure. Lastly, the sample was sintered in a hot press system up to 1400°C temperature and Argon atmosphere. Before testing, the sample was polished. Electrical conductivity was measured using four-probe method under air atmosphere and room temperature. The addition of Al₂O₃ decreased the overall electrical conductivity, but it did not decrease very much and could be used with wire electrode cutting. At 5 vol% Al₂O₃, the conductivity was $3.05 \cdot 10^6$ S/m and $2.56 \cdot 10^6$ S/m at 25 vol%. In Fig. 7, a dependence of electrical conductivity to the amount of vol% Al₂O₃ added to Ti₃AlC₂ is shown. A linear decrease in electrical conductivity is seen [4].

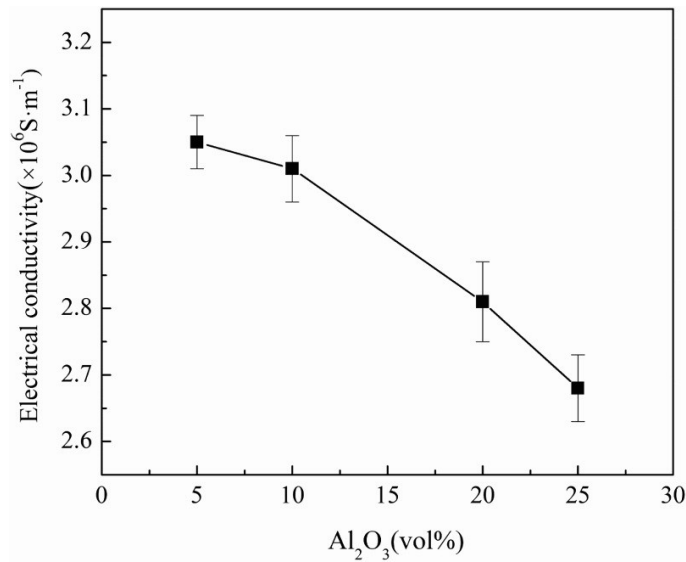


Fig. 7. Electrical conductivity dependence on vol% Al₂O₃ [4]

Other research measured electrical properties of Ti₃AlC₂ composite. The composite was produced by solid-liquid synthesis and in situ hot pressing. The starting Ti, Al and graphite powders were ball milled in ethanol for 12 hours. Later the composition was dried and formed into pellets in die under 30 MPa pressure. Then the pellet was sintered in vacuum at 1400°C temperature for 2 hours. The electrical conductivity was measured with dc four-probe method. It was measured that hot pressed Ti₃AlC₂ had a resistivity of 8.2·10⁻⁶ Ωm. Electrical conductivity is slightly higher than in other studies. Also, electrical conductivity was measured for Ti₃AlC₂/SiC and Ti₃AlC₂/ZrO₂ composites, which significantly increased the resistivity [20]. In table 1, comparison of the composite materials is shown.

Table 1. Comparison of Ti-Al-C composites properties

Material	Electrical conductivity, S/m	Electrical resistivity, Ωm	Measurement environment	Measurement method	Manufacturing method	Reference
TiC - 10 wt%Ti ₃ Al	1.2·10 ⁵	8.3·10 ⁻⁶	800 °C, air atmosphere	Kelvin 4 wire with AC resistance bridge	Pressure less sintering at 1500 °C	[10]
Ti ₂ AlC and Ti ₃ AlC ₂	1.85·10 ⁶	0.54·10 ⁻⁶	-	Linear Van der Pauw	Magnetron sputtering, annealing at 850 °C	[11]
Ti ₂ AlC - 5 wt% TiC	1.63·10 ⁶	0.613·10 ⁻⁶	20 °C, air atmosphere	Four-probe	Sintering at 1350 °C	[3]
Ti ₃ AlC ₂ – 5 vol% Al ₂ O ₃	3.05·10 ⁶	0.327·10 ⁻⁶	air atmosphere, room temperature	Four-probe	Sintered at 1400°C	[4]
Ti ₃ AlC ₂	1.22·10 ⁵	8.2·10 ⁻⁶	-	DC four-probe	Sintered in vacuum at 1400°C	[20]

The lowest resistivity seen was 0.327·10⁻⁶ Ωm and highest 8.3·10⁻⁶ Ωm. Most of the measurements performed with four-probe method under room temperature and air atmosphere.

1.3. Review of electrical conductivity measurement designs

In this chapter several patents and designs will be analyzed and reviewed. The first design is shown in Fig. 8. This design is intended for the measurement of semiconductor wafers.

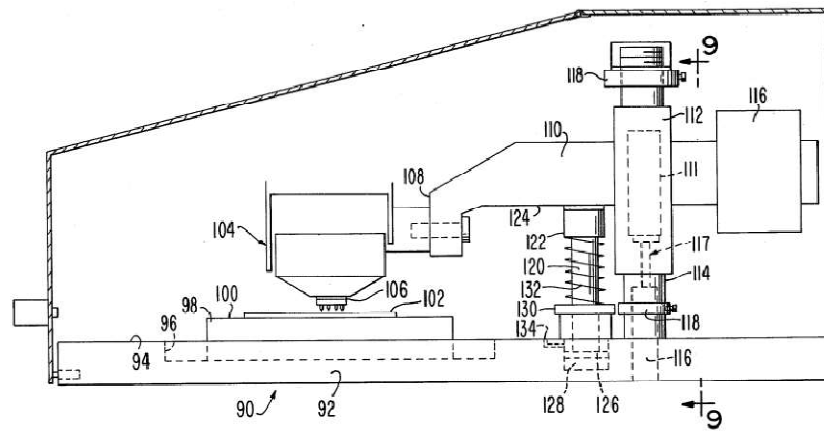


Fig. 8. Collinear four point probe design for resistivity measurement [21]

Here the numbers shown in Fig. 8 will be explained: 90 – Stand; 92 – Base plate; 94 – upper surface; 96 – Recess; 98 – Chuck; 100 – Upper feat surface; 102 – Semiconductor wafer; 104 – Probe head; 106 – Probe; 108 – Vertically shiftable arm; 110 – Means for lowering and raising arm; 111 – Cross beam; 112 – Vertical tubes; 114 – Upright post; 116 – Counterweight; 118 – Adjustable stops; 120 – Vertical shaft; 122 – Head; 124 – Lower surface; 126 – Piston; 128 – Cylindrical recess; 130 – Seal; 132 – Coil spring; 134 – Air inlet [21].

The measurement instrument can be adjusted in horizontal direction and vertical direction. An option can be made to have multiple probes for multiple resistivity measurements. The probe head can be lower by using pneumatic or hydraulics. The coil spring brings the probe head back up after measurement. A counterweight is used because measurement instrument is protruding from one side. The semiconductor sample is placed in an adjustable chuck to prevent movement [21]. A second design is shown in Fig. 9.

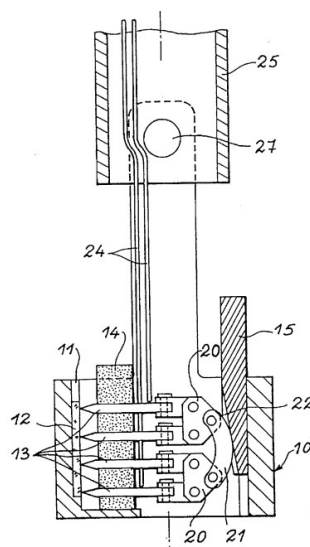


Fig. 9. Apparatus for measuring surface resistance and resistivity at high temperature [22]

Here the numbers shown in Fig. 9 will be explained: 10 – Measuring cell; 11 - Sample cavity; 12 – Sample; 13 – Electrodes; 14 – Insulating block; 15 – Wedge; 20 – Two brackets; 21 – End fitting; 22 – Groove; 24 – Electric leads; 25 – Suspension tube; 27 – Spindle [22].

Knife-like electrodes are contacting a sample that is placed in a dedicated area. Electrodes are placed and guided by an insulating block. Force to the knives is exerted by a beveled shim. This shim is pushed by gravity. Whole system can perform measurements in very high temperatures. Current and voltage leads are put into a suspension tube from ceramic to be able to withstand high temperatures. Such design is limits the sample geometry because cavity for sample is not adjustable [22]. In Fig. 10, a third design is show. This apparatus is also intended to be used in high temperature environment.

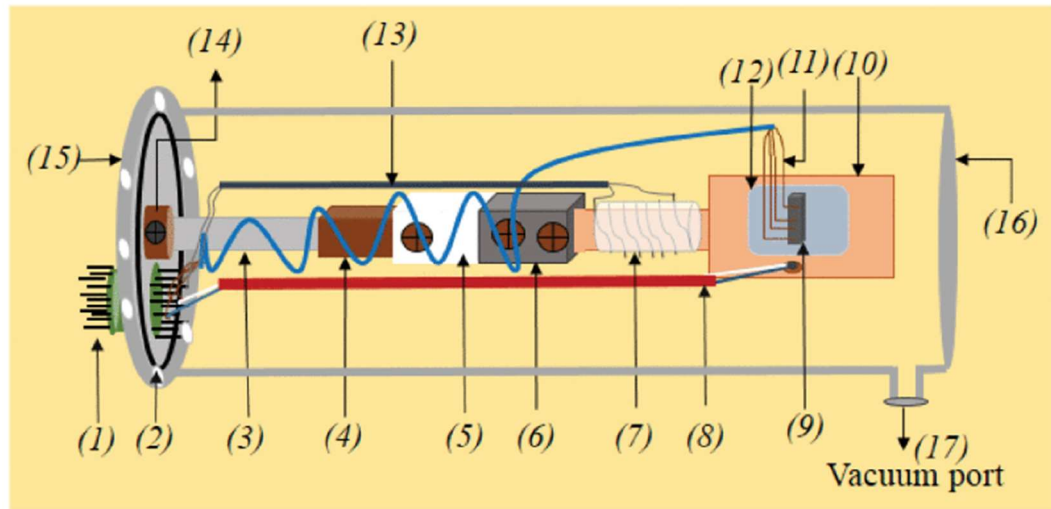


Fig. 10. Apparatus for resistivity measurement in high-temperature range [23]

Here the numbers shown in Fig. 10 will be explained: 1 – Electronics block; 2 – Circular ring; 3 – Stainless steel rod; 4 – Brass rectangular bar; 5 - Rectangular Teflon bar; 6 - Rectangle gypsum bar; 7 – Heater; 8 – Thermocouple; 9 – Sample; 10 – Rectangular copper plate; 11 – Coating of insulation; 12 – Thin mica sheet; 13 – Copper wire; 14 – Circular brass disc; 15 – Flange; 16 – Vacuum tube; 17 – Vacuum port. [23].

The sample is placed on a sheet of mica sheet. Mica sheet is a good thermal conductor and a good electrical insulator. The mica sheet is placed on top of the copper plate, which is heated. Silver paste is used to further increase thermal conduction. Heat is transferred to the sample. The heater attached to the end of the copper plate is heating it by thermal conduction. Resistive heating is used by the heater. The heater has kanthal wires inside, which has 35 Ω resistance. Two copper wires coming from the electronic block is supplying current to the heater. A thermocouple is measuring temperature on the copper plate. Both thermocouple and four measurement wires are connected to electronic block which is hermetically seals. The whole apparatus is enclosed in vacuum tube. Vacuum is supplied by vacuum pump that is connected to the port. A gypsum bar is located at the end of copper bar to prevent heat dissipation. Gypsum has a very low thermal conductivity. Teflon bar, brass bar and steel rod are needed for mechanical support. Flange seals the vacuum tube [23].

2. Methodology for selecting electrical conductivity measurement principle

Before selecting the method, the tested material must be analyzed. The tested samples have a cylinder pellet shape, variance from approximately 10.05 to 10.35 mm diameter and 4.75 to 6.45 mm thickness. Samples does not have a perfect shape, variations in thickness and diameter occurs throughout the geometry. The composite sample has a metal matrix with carbides and MAX phase reinforcement. Resultant composite has properties found in metals and ceramic materials. The composite is produced from powders. To achieve good homogeneity throughout the sample, the powders must be mixed very well. HVED (high voltage energy discharge) technique was used in kerosene liquid. During HVED kerosene pyrolysis and synthesis of carbon nano particles occurs. After HVED process, the powder mixture of metal matrix, carbides, MAX phases, and carbon nano particles are solidified by using SPS (spark plasma sintering) method. The surface of the sample is polished, but due to the nature of the production method surface roughness and porosity still exists on the surface. In table 2, the geometrical parameters of the samples are shown.

Table 2. Geometrical parameters of samples

Sample	Diameter, mm	Thickness, mm
N6	10.35	4.75
N7	10.1	6.45
N8	10.05	5.6
N10	10.1	6.4
G6	10.1	5.5
G7	10.2	4.9

There are six samples with different compositions.

2.1. Selection of electrical conductivity measurement method

Traditional resistivity measurement methods use two probes, but this method includes the contact resistance of the probes. By using four probes the contact resistance is eliminated. Two common arrangements of the four-probe method is the collinear, when all probes are arranged in one line and the Van der Pauw arrangement when probes are evenly spaced at four corners of the sample [7]. One of the main conditions for the Van der Pauw method is even thickness throughout the sample, which is not fulfilled in this case. Also, making an adaptable mechanism for different diameter samples, that contact the edge could be challenging. In addition, other reviewed experiments for similar samples used the collinear four-probe method. The collinear four-probe method can be adapted for such sample geometry. In this method, the outer two probes are driving current through the sample and the two inner probes are measuring voltage. It is very important for the individual probes to be spaced evenly. A condition for this method is small contact area or point contacts. Generally, needle type probes are used. Such probes have very small contact area and can ensure proper contact to sample, puncturing any oxide layer on the surface [7]. Additionally, spring loaded probes allows equal contact between all the probes.

Because of the current paths of the two outer probes, the sample size and geometry influence the result. If the sample is large in width and thickness, all current paths can flow freely, however, if sample is small so that the current paths are obstructed, measurement is influenced. In Fig. 11, the current paths of a semi-infinite 3D material are shown [7].

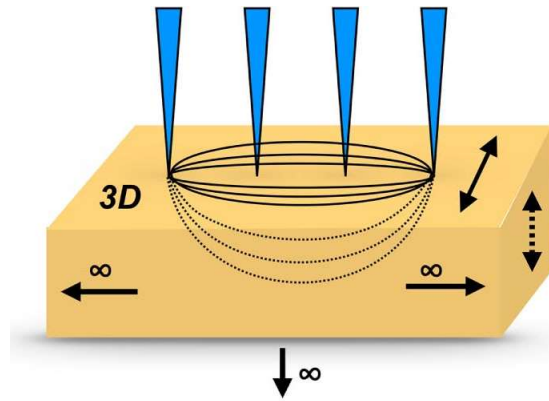


Fig. 11. Current path of semi-infinite 3D material [7]

Current paths can be seen both on the surface and inside of the material. Infinite dimensions in length, width and height do not obstruct current paths. The current paths can be made smaller by reducing the distance between the probes. To eliminate errors coming from the finite geometry, correction factors are used. There are three types of correction factors, F1 coming from finite thickness of the sample, F2 position of the probes in relation to the sample edge and F3 finite lateral width of the sample. If ratio between thickness and probe spacing is more than 4, it can be considered as having infinite thickness and correction factor for thickness would not be needed. The probe spacing should be selected based on this condition. If the probes are arranged at least four probe spacings from the side of the sample, correction factor F2 is not needed [7]. If the sample diameter ratio with probe spacing is over 40, the correction factor F3 is not needed [24]. Because of these factors it's important to position the probes in the middle of the sample. Another important characteristic is the isotropy or anisotropy and homogeneity of the sample. Homogeneity throughout sample is fulfilled by the HVED method. It is observed by other research that metal matrix composites manufactured from powders and do not have a fiber reinforcement are isotropic [6].

2.2. Electrical conductivity measurement environment conditions

Electrical conductivity measurements are affected by environment conditions, these are temperature, relative humidity and atmosphere. Biggest factor is temperature especially when measuring metals that are good thermal conductors. Metals electrical conductivity decreases when it is heated and increases when it is cooled. This can be explained by the increase of electrons bouncing in higher temperature which makes it harder for electricity to flow. In material science, the temperature dependence on electrical conductivity is very important. Many similar research use heating elements/chambers to get the temperature-resistivity characteristic [18, 23]. However there are few measurement set ups with cooling capability. A peltier module has the capability to heat and cool. A thermoelectric module or peltier module used the peltier effect. When current is applied to the module one side is heated and the other is cooled. The cooling/heating sides can be reversed by reversing current polarity. A peltier module has a temperature rating which shows the temperature difference between the two sides. By increasing or decreasing temperature in one side, the opposite side can increase/decrease temperature by the same amount. To reach a lower temperature when cooling is used, a heat sink element could be used on the hot side. Temperatures below freezing and around 100 °C could be achieved depending on the module. The peltier module would need to touch the sample, since most of the temperature would be transferred with conduction. To increase the contact area

between sample and peltier module thermal paste is applied. Thermal paste fills the irregularities and rough parts which increases surface area. Thermal paste and the peltier module are from insulative material, so they don't influence the measurement. A peltier module is a very simple and compact way of heating/cooling that doesn't require very complicated devices. However, small temperature range can be achieved.

Another important aspect is the relative humidity and atmosphere. Humidity in the air can affect sample with moisture and oxidation. Excess moisture can create water layers which increase the electrical conductivity. Other studies show a decrease in resistivity with increasing relative humidity [25]. Oxidation is another negative affect especially when measuring metals. Humidity increases oxide layer formation, which is non conducting. To eliminate the negative effects of humidity, measurements should be made in vacuum. Additionally vacuum would reduce convective heat losses [23]. Measurements in vacuum are more repeatable and comparable with other studies.

2.3. Current source and voltage measurement selection

The current used in the outer probes must not heat the sample or the probes. It is known that higher temperature increases the resistivity, this influences the final result. To prevent or minimize heating of the sample and probes, current source must be pulsed DC or AC type. If constant DC current is used Joule heating is induced. When using pulsed DC or AC type current, voltage measurement is made quickly before heating occurs. A small current should be selected if constant DC is used. For pulsed DC or AC, higher current can be used. Measurements with higher current gives a more accurate result because resultant voltage will be higher. Higher voltage can be measured more accurately. Another source of error comes from the thermoelectric effect, this can be negated by measuring with forward current and reversed current. An average of the two measurements will give a value without the thermoelectric effect influence [23].

When measuring the electrical conductivity of metals or very conductive material, a nanovoltmeter is needed. Measurement of small voltage is subjected to outside influence, such as: electromagnetic fields from other devices, static electricity, improper grounding. Coaxial cables can be used to protect from outside influence or measurement in a controlled environment such as vacuum.

2.4. Simulation of colinear four-point probe measurement

A simulation was performed to validate model and better understand current flow. A model was created with Comsol software. Cylindrical sample has 6 mm height and 10 mm diameter. Two adjacent probes are spaced 2 mm apart. Probe spacing is chosen based on the needles and the biggest diameter of the sample. Probe needle tip is not infinitely small, the tip is 0.04 mm diameter. The tip had to be of finite diameter because very small mesh would be needed. Model is shown in Fig. 12.

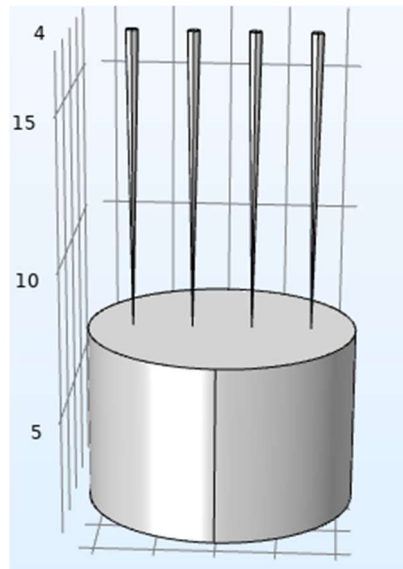


Fig. 12. Sample and probe arrangement model in COMSOL

Electric currents, Joule heating and solid mechanics physics are used in the simulation. Sample and probes are separate entities and form an assembly. Mechanical and electrical contacts are applied to areas where probes touch sample. One probe current is applied point current source of 1 ampere. The other current probe is given ground. Sample is given pure Titanium material properties because it's the closest material to real samples available. At the positions of the voltage probes, electric potential values are taken. The plot of the simulation can be seen in Fig. 13.

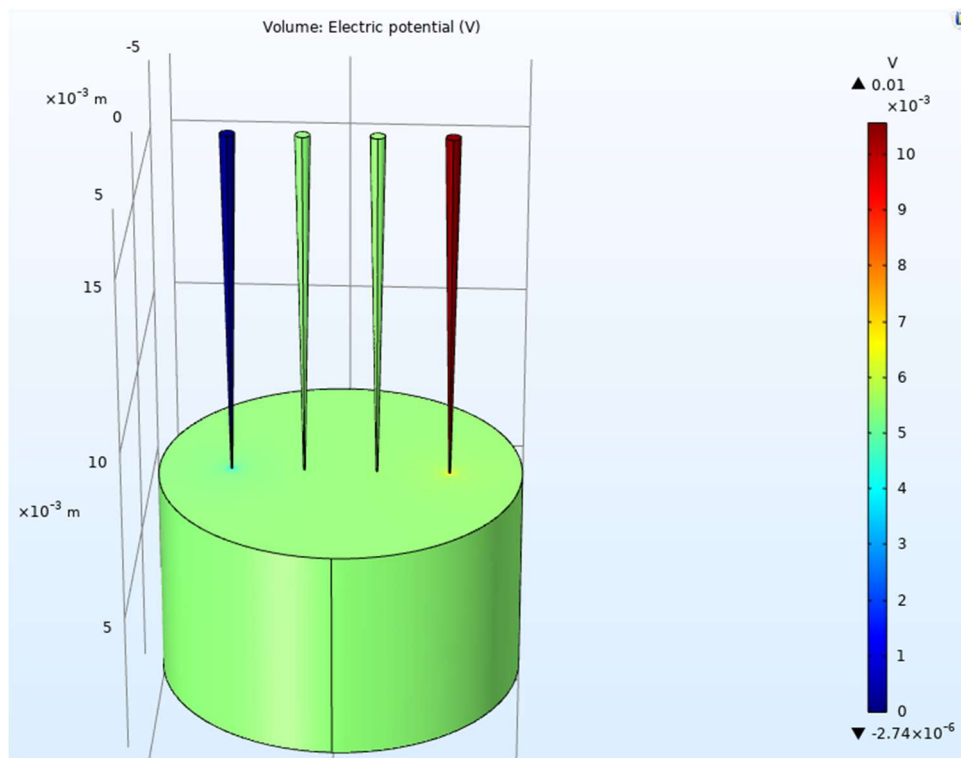


Fig. 13. Electric potential plot of collinear for point probe method from COMSOL

It can be seen from the 3D plot that the current paths distribute around the sample and get cut off at the sides. It is well known that finite geometry samples resistivity measurements need correction factors [7]. The potential difference between the two probes is calculated by using Eq. 1.

$$U = U_1 - U_2 \quad (1)$$

where: U_1 is the potential of the first probe (V); U_2 is the potential of the second probe (V); U is the potential difference (V).

$$U = 3.92 \cdot 10^{-3} - 3.88 \cdot 10^{-3} = 3.8 \cdot 10^{-5} \text{ V}$$

The resistivity without correction factor is calculated by using Eq. 2.

$$\rho = 2 \cdot \pi \cdot s \cdot \left(\frac{U}{I}\right) \quad (2)$$

where: ρ is the resistivity of the sample material ($\Omega \cdot \text{m}$); s is the spacing between two adjacent probes (m); I is the current applied between current probes (A).

$$\rho = 2 \cdot 3.14 \cdot 0.002 \cdot \left(\frac{3.8 \cdot 10^{-5}}{1}\right) = 4.77 \cdot 10^{-7} \Omega \cdot \text{m}$$

Resistivity with correction factor is calculated by using Eq. 3. Two correction factors applied that are taken from literature [26].

$$\rho_c = 2 \cdot \pi \cdot s \cdot \left(\frac{U}{I}\right) \cdot F_1 \cdot F_2 \quad (3)$$

where: ρ_c is the resistivity of the sample material with correction factors ($\Omega \cdot \text{m}$); F_1 is the correction factor for finite thickness; F_2 is the correction factor for finite lateral width.

$$\rho_c = 2 \cdot 3.14 \cdot 0.002 \cdot \left(\frac{3.8 \cdot 10^{-5}}{1}\right) \cdot 0.978 \cdot 0.7419 = 3.46 \cdot 10^{-7} \Omega \cdot \text{m}$$

The true resistivity of Titanium presented in Comsol is $3.846 \cdot 10^{-7} \Omega \cdot \text{m}$. Resistivity with correction factor is closer to the true value of the material. The percentage error with correction factor is 10% and 24% without correction factor.

2.5. Simulation of probes contact force to sample

A simulation was performed to determine the influence of contact force to the electrical connection of probes and sample. Contact pressure parameter was applied to the contact pair at the connection area. Ideally probe tip should be infinitely small, in this case probe tip had radius of 0.02 mm and area of $1.25 \cdot 10^{-9} \text{ m}^2$. The needle probe used in setup will be spring loaded and will have a force rating. By using Eq. 4, contact pressure can be calculated.

$$P = \frac{F}{A} \quad (4)$$

where: P is the contact pressure (N/m^2); F is the theoretical force of spring-loaded probe (N); A is the area of probe tip (m^2).

Contact pressure is calculated for all four probes:

$$P_8 = \frac{4.8}{4 \cdot 1.25 \cdot 10^{-9}} = 6.39 \cdot 10^9 \text{ N}/\text{m}^2$$

Simulation results are presented in Table 3:

Table 3. Contact force simulation results

Contact pressure applied to all four probes, N/m ²	Force on individual probe, N	Resistivity no correction, Ωm	Resistivity with correction, Ωm
$3.99 \cdot 10^9$	5	$2.69 \cdot 10^2$	$1.95 \cdot 10^2$
$6.39 \cdot 10^9$	8	$4.77 \cdot 10^{-7}$	$3.46 \cdot 10^{-7}$
$7.98 \cdot 10^9$	10	$4.77 \cdot 10^{-7}$	$3.46 \cdot 10^{-7}$

It was found that at least 8 N force is required to have adequate contact. If force is increased further, no change is seen. The resistivity at 8 N force or higher is the same as bonded connection. Below 8 N force, big variation is seen. Resistivity is much smaller than true value. This indicates that proper connection between probe and sample is not made. This behavior can be due to surface roughness and hardness of the materials. At a certain force, in this case at 8 N, surface roughness is flattened and an ohmic connection is made.

In Fig. 14, a plot of von Mises stress is shown. During shown simulation 8 N force or $6.39 \cdot 10^9$ N/m² is applied. The probes were constrained in X and Y directions. The sample was fixed immovably.

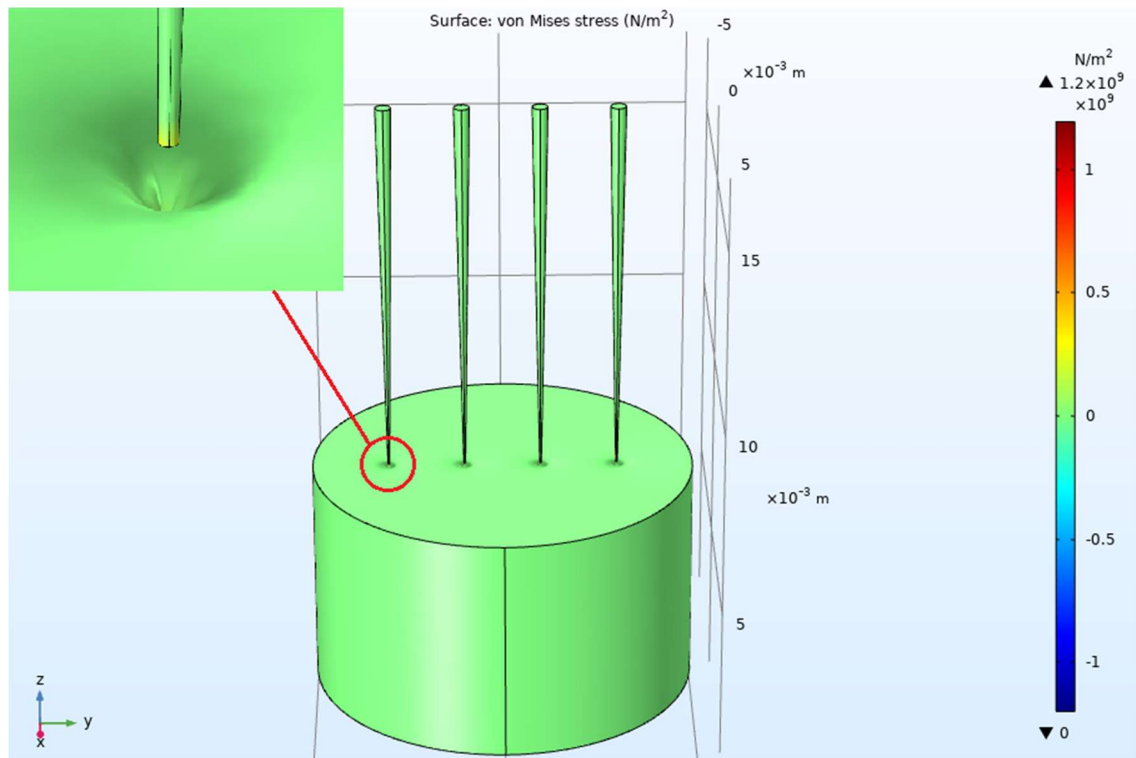


Fig. 14. von Mises stress plot with 8 N force applied

Biggest stresses are in the tip of the probe needle. The probe is given copper material properties. Maximum 1.2 GPa is seen at the very tip, which is higher than coppers yield strength. The stress in the sample is lower than the yield strength of titanium. In this simulation copper probes would get bent and damaged, but titanium sample would not. In real scenario, the probe needles would have much sharper tip and lower force would be needed to achieve ohmic contact. However experimental testing would be needed to find the minimum needed force.

3. Development of electrical conductivity measurement setup

In this part the design and fabrication process of the electrical conductivity measurement setup will be presented.

3.1. Modeling of electrical conductivity measurement setup

The measurement setup had to meet these conditions:

1. It had to fit and hold a 10.05 to 10.35 mm diameter and 4.75 to 6.45 thickness pellet shape sample that is of irregular shape.
2. It had to fit into a vacuum chamber which had a 150 mm width, 250 mm length and 360 mm height.
3. It had to be open so that vacuum can get in.
4. The test probes had to be small enough to measure the sample.
5. It had to be able to cool or heat the sample.

For measurement a collinear four-point probe method was selected as discussed in previous chapter. Needle like test probes were selected due to requirements of the method and small sample. An Ingun spring loaded test probe with sharp tip was used. For heating and cooling, a Peltier module TEC1-19906 was used, it had 40 x 40 x 4 mm geometry. The Peltier element could achieve a maximum temperature of 83 °C and a minimum temperature of -55 °C.

A sample holder was designed as show in Fig. 15. In the middle it had an egg-shaped hole for placing the sample. Such shape allows to position the sample accurately and only one fixation screw is needed. The sample is contacted with two lines and one point, two lines from the edges of the egg-shape holder and one point by screw tip. The two-line contact positions the sample vertically.

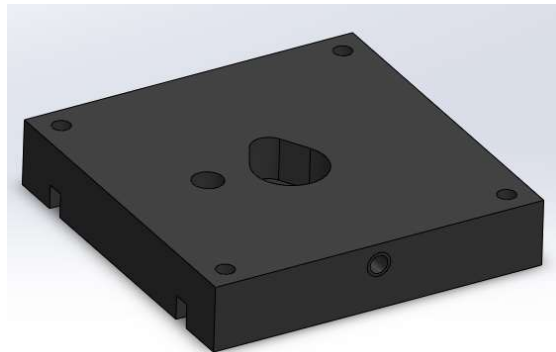


Fig. 15. Model of sample holder

Screw used to fix the sample was from insulative plastic, so that it cannot influence the measurement. The bottom of the holder had a 40 mm width, 40 mm length and 4 mm square shape opening for putting in the Peltier module. A pathway for the Peltier elements wires was also made. Furthermore, a hole of 5 mm was made for the temperature sensor to monitor the Peltier elements temperature. The sample holder itself is fixed into a cooling element by four bolts. Material of the sample holder must be from insulative plastic to not influence measurement.

The second part was the cooling element. It is shown in Fig. 16. The cooling element is from aluminum and is used to receive heat from the Peltier module by thermal conduction, it acts as a

heatsink. Peltier module is held by and fixed to the cooling element by the sample holder. Thermal paste is applied between the cooling element and Peltier module to improve the thermal conduction.

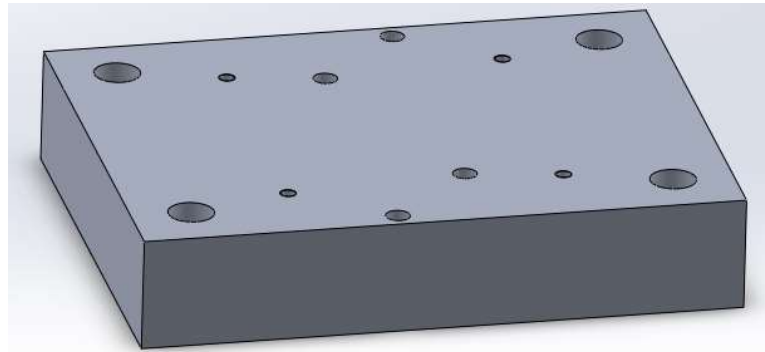


Fig. 16. Model of cooling element

The cooling element also acts as a linear movement transmission. It has four holes at the corners where cylindric guides are positioned. It can move up and down vertically. The four guides keep the cooling element horizontal to the surface while moving. The clearance between the holes and cylinder must be so that sliding is permitted, but there is no tilting. The linear guides and holes should be lubricated with oil to reduce friction. Movement is actuated by linear drive mounted below the cooling element. Linear drive and cooling element are connected by brackets and bolts.

A separate part was designed for holding the needles. It has four holes in the middle. The needles will be pressed into the holes, so they must be slightly smaller than the needles. The needle diameter is 1.35 mm. Adjacent needles have 2 mm distance. A separate part for needle holders were made because of easy replacement in case needles get broken. In Fig 17, the model of the needle holder can be seen.



Fig. 17. Model of needle holder

The needle holder is of cylindrical shape to allow rotation of the holder and in turn the needles. This design choice allows to measure the sample at different angles. Two holes for bolts are made at the top of the sample to make it easier to rotate by hand and if needed to take it out. The bolts at the top of the holder also give some protection form damage. Holder is held by a circular fixation element, which also provides some protection to the top of the needles. The material of the needle holder is from insulative plastic to prevent short circuit.

A full assembly of the measurement setup is shown in Fig. 18. The housing of the setup consists of top part, bottom part and four cylindrical rods. The top and bottom housing parts are from plastic and

rods are from anodized aluminum. The top housing part has a stepped hole which perfectly fits the needle holder. There are three tapped holes for fixation part from top side. In addition, four tapped holes are from bottom side for the linear guides. The linear guides have a threaded end, which screws into the top housing.

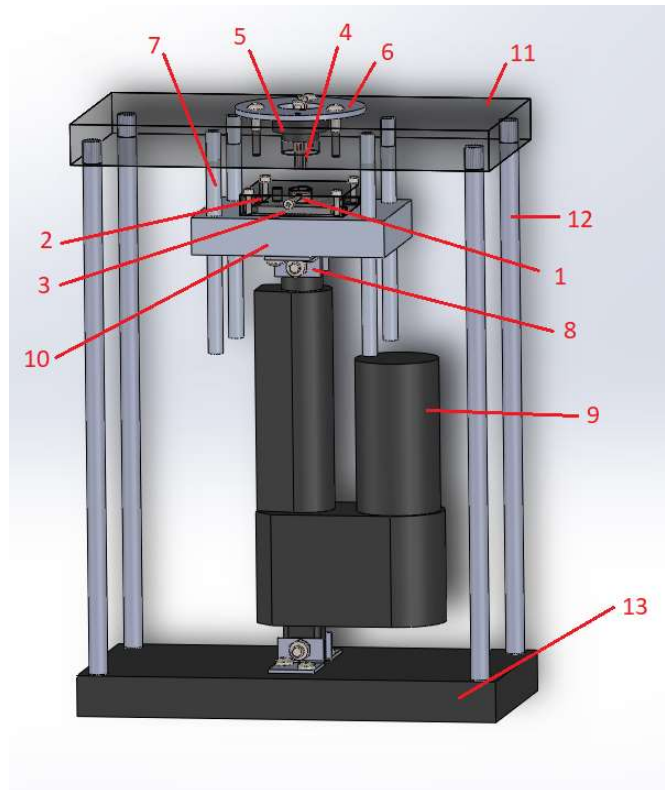


Fig. 18. Electrical conductivity measurement setup Solidworks model: 1 – Sample; 2 – Sample holder; 3 – Peltier element; 4 – Test needles; 5 – Needle holder; 6 – Fixing element; 7 – Linear guides; 8 – Bracket; 9 – Linear motion drive; 10 – Cooling element; 11 – Top housing; 12 – Housing rod; 13 – Bottom housing.

The bottom housing part has the same width and length as the top part. Furthermore, it has a square pocket which positions the linear drive. Also, there are tapped holes for brackets which connect the bottom housing with linear drive. Both housing parts are connected through cylindrical rods. Holes are made at four corners of both housing parts that fit the aluminum rod. Cylinder and housing holes have a pressed fit. The full width of the setup is 120 mm, length – 228 mm and height – 323 mm. It fulfills size requirement for fitting into vacuum chamber. The maximum sample diameter is 11 mm, minimum diameter 7 mm. Minimum sample height is 4 mm, maximum sample height could be up to 20 mm.

The sample is placed in sample holder with thermal paste applied on the side which touches the Peltier module. The thermal paste has two functions, increasing surface area and allowing the sample to lay flat despite thickness irregularities. Sample movement is from bottom up because it prevents bending of needles due to surface roughness and irregularities of the sample. The cylinder has a 50 mm travel and travel speed of 3 mm/s. Only 10 to 15 mm travel distance is needed depending on sample thickness. The cylinder travel is controlled by Arduino board. The test needles are spring loaded by 2N springs and have a sharp tip that can penetrate oxide layer. The samples are placed by tweezers. Before sample can be putted in or taken out, needle holder must be taken out. In Fig. 19, a cross section view of the set up shown.

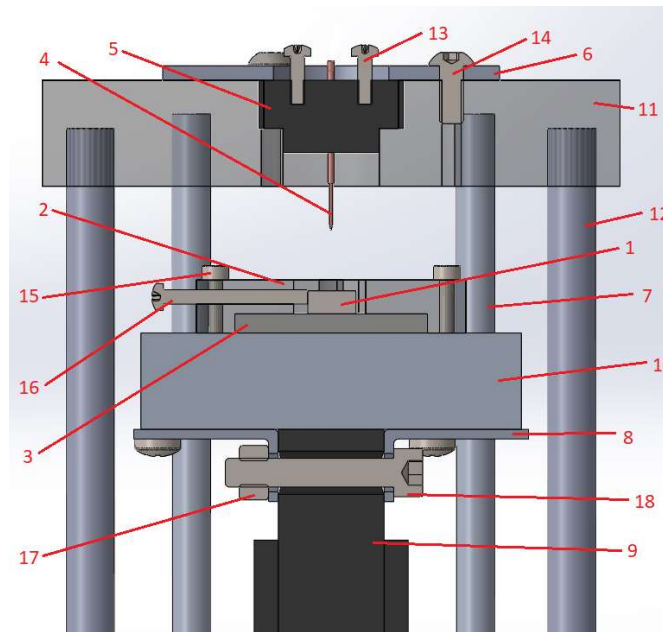


Fig. 19. Electrical conductivity measurement setup cross section view: 1 – Sample; 2 – Sample holder; 3 – Peltier element; 4 – Test needles; 5 – Needle holder; 6 – Fixing element; 7 – Linear guides; 8 – Bracket; 9 – Linear motion drive; 10 – Cooling element; 11 – Top housing; 12 – Housing rod; 13 – ISO 7045 M3 x 10 bolt; 14 – ISO 7380 M5 x 12 bolt; 15 – ISO 4762 M3 x 25 bolt; 16 – ISO 7045 M3 x 30 bolt; 17 – ISO 4034 M6 nut; 18 – ISO 4762 M6 x 35 bolt.

In the cross-section, bolt connections can be seen. All bolts and nuts are standard ISO parts. All tapped holes have standard pitch.

3.2. Fabrication of electrical conductivity measurement setup

First part that was produced was the sample holder. A block of polypropylene of 60 x 60 x 120 mm dimensions was used as raw material. The process of fabricating the sample holder is presented in Table 4.

Table 4. Sample holder fabrication process

Operation	Used tool	Used equipment
Cutting raw material to 56 x 56 x 12 mm square part	Slide mill cutter	Disc mill cutter
Milling a pocket of 40 x 40 mm square to 4 mm depth	End mill 4 mm	Milling machine
Cutting 3 mm width and 4 mm depth groove	Slide mill cutter	Disc mill cutter
Drilling through 12 mm and 6 mm holes to for egg-shaped hole	12 mm and 6 mm drill bit	Vertical drilling machine
Milling to form egg-shaped hole	End mill 3 mm	Milling machine
Drilling four through 3 mm holes at the corners	3 mm drill bit	Vertical drilling machine
Drilling through 5 mm hole for temperature sensor	5 mm drill bit	Vertical drilling machine
Drilling through horizontal hole M4	3.3 mm drill bit	Vertical drilling machine
Tapping M4 hole	M4 tapping tool	-
Grinding and deburring uneven edges	File, sandpaper	

In Fig. 20 a fully fabricated sample holder is shown. It is also equipped with M4 plastic bolt and Peltier module.

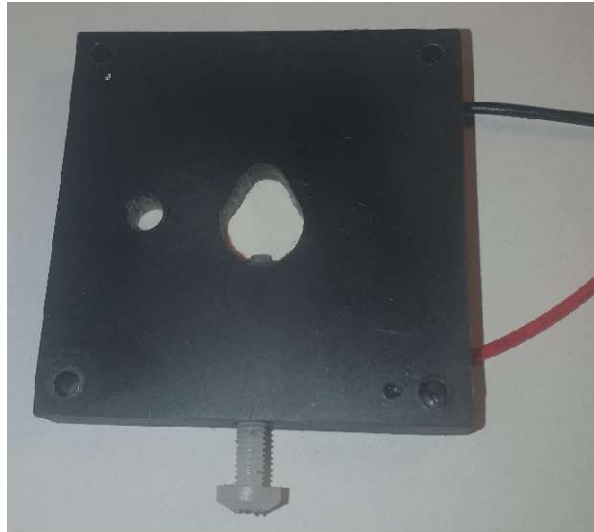


Fig. 20. Fabricated sample holder

Milling a straight tangent line for the egg-shaped hole was impossible. A file and sandpaper used to get final shape. Groves for Peltier module wires had to be made on both sides of the holder due to rounded edges that were formed during milling of pocket.

Second part that produced was the needle holder. A cylinder block of 40 mm diameter polypropylene was used as raw material. The process of fabricating the sample holder is presented in Table 5.

Table 5. Needle holder fabrication process

Operation	Used tool	Used equipment
Turning cylinder to 28 mm diameter, 17 mm distance	Turning tool	Lathe machine
Turning cylinder to 20 mm diameter, 5 mm distance	Turning tool	Lathe machine
Cutting 17 mm distance	Cutting tool	Lathe machine
Turning until 15 mm thickness is reached	Turning tool	Lathe machine
Drilling four through 1.35 mm holes	1.35 mm drill bit	Vertical drilling machine
Drilling blind 2.5 mm hole	2.5 mm drill bit	Vertical drilling machine
Tapping M3 holes	M3 tapping tool	-

In Fig. 18 a) needle holder after turning process is shown. Part had to be taken out and turned again until it fit perfectly with hole in top housing. Fig. 21 b) shows needle holder fully assembled. Needles had to be pressed into holes by using a press. Before pressing, needles and hole were lubricated with oil to prevent bending of the needles. Wires were soldered into top of the needles.

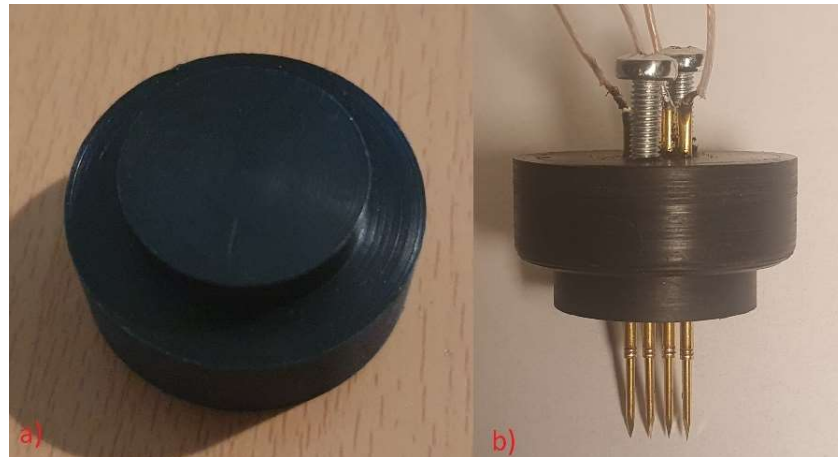


Fig. 21. Needle holder, a) after turning; b) finished part

Fabrication of cooling element, heatsink is shown in Table 6. An aluminum block 100 x 100 x 20 mm was used as raw material.

Table 6. Cooling element fabrication process

Operation	Used tool	Used equipment
Cutting block to 100 x 80 x 20 mm	Slide mill cutter	Disc mill cutter
Drilling four through 8 mm holes	8 mm drill bit	Vertical drilling machine
Drilling four blind 2.5 mm holes	2.5 mm drill bit	Vertical drilling machine
Drilling four through 4.2 mm holes	4.2 mm drill bit	Vertical drilling machine
Tapping M3 holes	M3 tapping tool	-
Tapping M5 holes	M5 tapping tool	-
Chamfering 8 mm holes from both sides	20 mm mill	Milling machine

In Fig. 22 a) the aluminum block is shown after cutting and b) after all the operation has been completed.

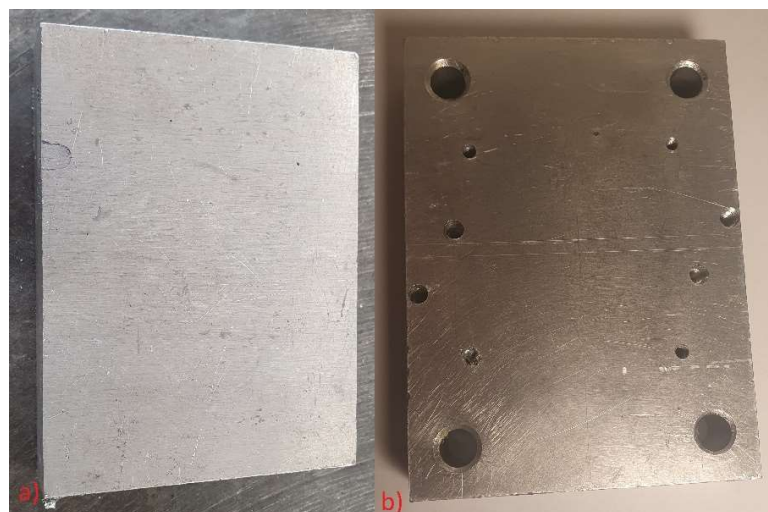


Fig. 22. Cooling element, a) after cutting; b) finished part

It was important to get accurate positions of the 8 mm holes because of the linear guides. Also, they were chamfered to prevent sticking and to keep oil on the chamfers. In addition, abrasive valve grinding paste was used while simulating sliding on the guides to make holes smoother. In real conditions oil is used to further improve sliding.

For top and bottom housing, a block of 230 x 320 x 22 mm of polypropylene was used. In Table 7, the fabrication process for top housing is presented.

Table 7. Top housing fabrication process

Operation	Used tool	Used equipment
Cutting width to 120 mm	Slide mill cutter	Disc mill cutter
Milling 20 mm through hole	End mill 20 mm	Milling machine
Milling 28 mm blind hole	End mill 28 mm	Milling machine
Drilling four blind 9.7 mm hole	9.7 mm drill bit	Vertical drilling machine
Drilling four blind 6.7 mm holes	6.7 mm drill bit	Vertical drilling machine
Tapping M8 hole	M8 tapping tool	-
Drilling three 4.2 mm blind holes	4.2 mm drill bit	Vertical drilling machine
Tapping M5 hole	M5 tapping tool	-

In Fig. 23, a picture of fully fabricated top housing with linear guides screwed in is shown. Linear guides were threaded manually by using a lathe. Only 15 mm was threaded.



Fig. 23. Top housing with linear guides

The housing rods were produced from two 1-meter aluminum rods. Turning cutting was used to cut them to required length. In Table 8, bottom housing fabrication process is shown.

Table 8. Bottom housing fabrication process

Operation	Used tool	Used equipment
Cutting width to 120 mm	Slide mill cutter	Disc mill cutter
Drilling four blind 9.7 mm hole	9.7 mm drill bit	Vertical drilling machine
Milling 20 x 20 x 3 mm pocket	End mill 8 mm	Milling machine
Drilling four through 4.2 mm holes	4.2 mm drill bit	Vertical drilling machine
Tapping M5 holes	M5 tapping tool	-

Bottom housing was fixed to the linear drive through brackets and an M6 bolt. A fully assembled measurement setup can be seen in Fig 24.

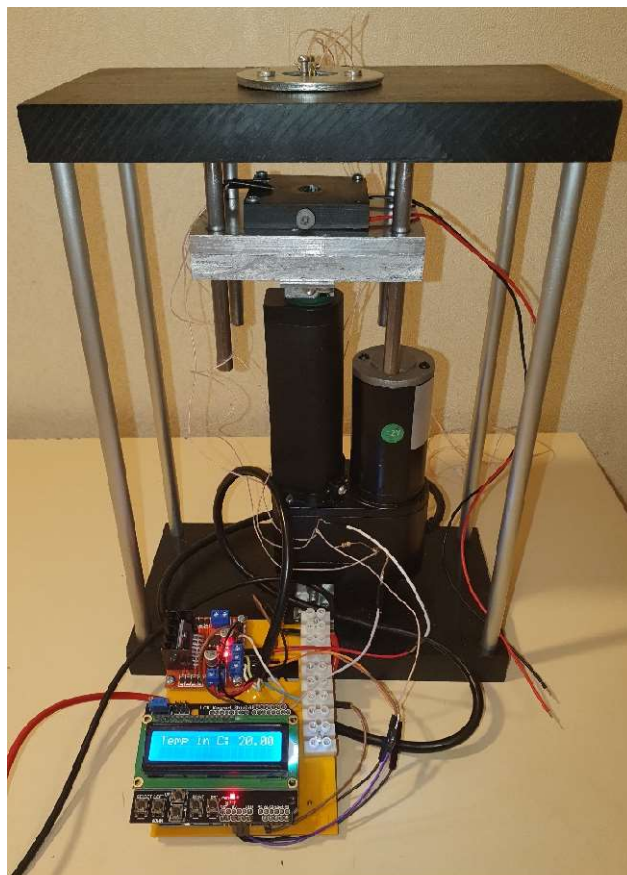


Fig. 24. Fully assembled measurement setup

A temperature sensor was made that contacts the Peltier element. An Arduino board was connected to LCD shield. Temperature reading can be seen in the LCD screen. A motor control module was also connected to the Arduino board for controlling the linear drive.

3.3. Control and electrical part of electrical conductivity measurement setup

In this part the electrical connections, control and their components will be discussed. In Fig. 25, a circuit of electrical part is shown.

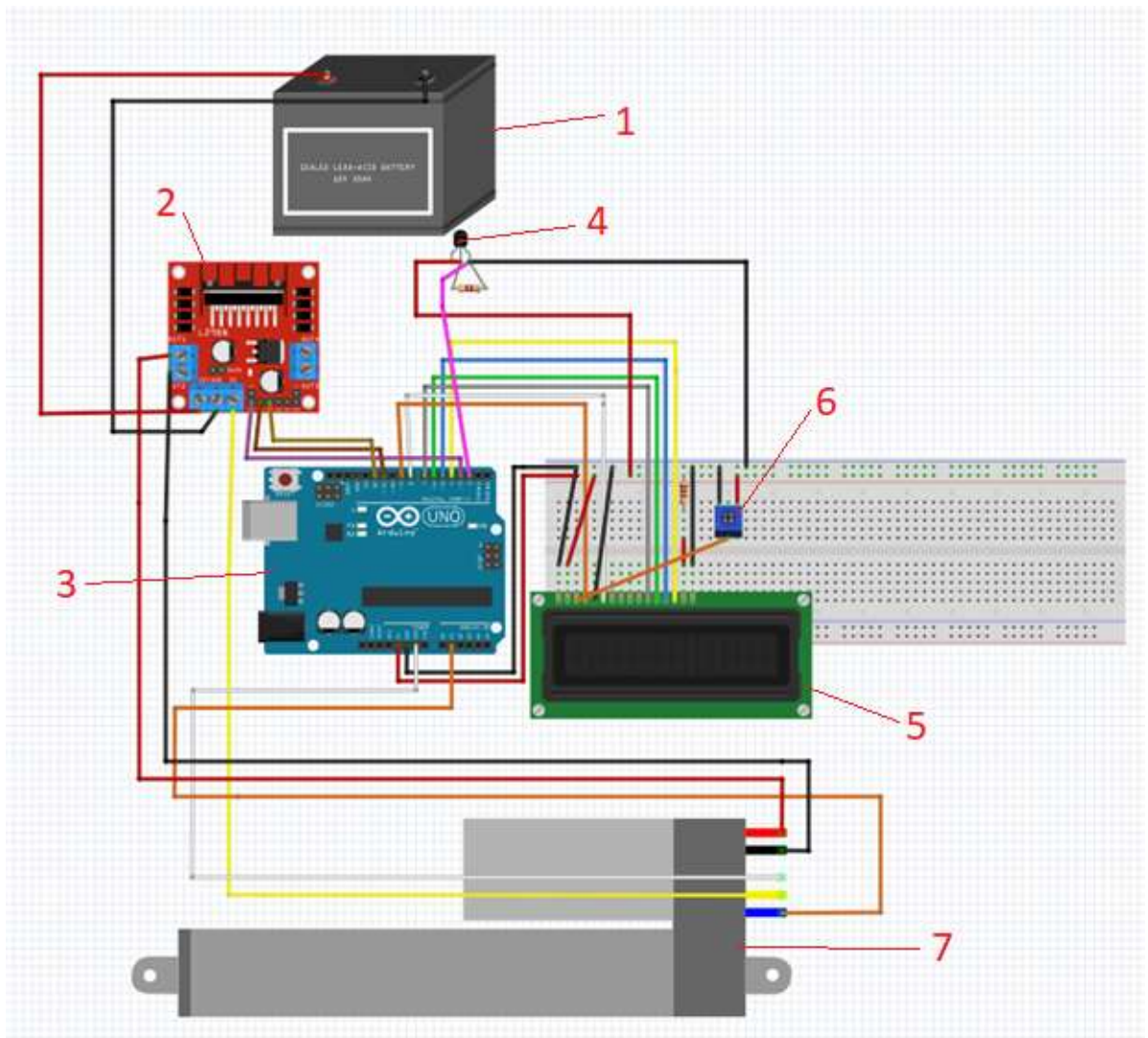


Fig. 25. Circuit of electrical part: 1 – 12V power supply; 2 – L298N motor driver; 3 – Arduino Uno; 4 – DS18B20 digital temperature sensor; 5 – LCD screen; 6 – Potentiometer; 7 – Linear drive.

The Arduino Uno is the central part of the control system. It is connected to the L298N motor driver, LCD screen and temperature sensor. The linear drive is controlled by L298N motor driver. Linear drive has a potentiometer with position feedback. It is operated by 12V, a 12V battery or power supply is required. Also, it has five wires. Red positive and black negative wires are used to supply current to the linear drive. They are connected to the L298N motor driver OUT1 and OUT2 connections. A motor driver is required because Arduino module cannot supply 12V on its own. The motor driver acts as a relay to control the linear drive. Power supply positive and negative wires are connected to the corresponding ports in L298N motor driver. White wire of the linear drive is connected to ground and yellow wire is connected to 5V port in the L298N motor driver. Potentiometer wire is connected to Arduino module to monitor cylinder stroke.

A 1602 2x16 LCD shield is used to show temperature from the temperature sensor. A DS18B20 digital temperature sensor is used to measure temperature. It has three wires; one wire is used for measuring. One outer wire is connected to ground and other outer wire to 5V. Middle wire is connected to one of the Arduino pins. A 4.7 k Ω resistor is connected in parallel between the middle and positive wire. The LCD screen has 16 connections. Four of the outer ports are connected to

4. Testing electrical conductivity of Titanium metal matrix composite samples

In this part the measurement setup was tested. Needles contacted the sample without breaking or bending. It contacted in the middle of the sample as intended in the design. Picture of cylinder in top position while needles are touching sample is shown in Fig 27.

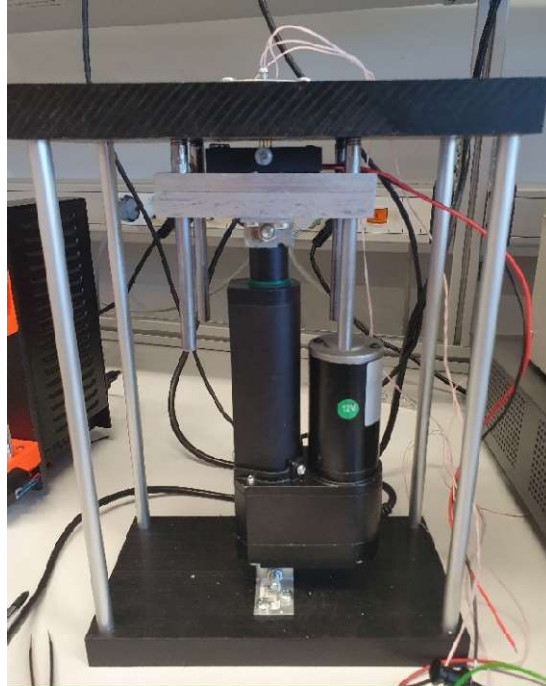


Fig. 27. Test needles contacting the sample

A Keithley 2614b source meter was used as a current source and voltage measurement tool. Voltage measurements were done with pulses. Number of measurements can be selected before test. A mean, standard deviation, minimum and maximum values were given by the meter. A picture of the Keithley 2614B source meter is shown in Fig. 28.

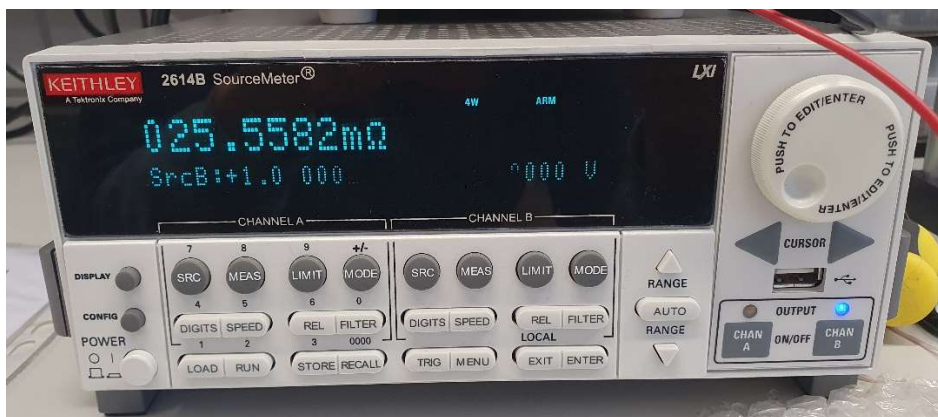


Fig. 28. Keithley 2614B source meter

Measurements were performed by using 4 wires and ohmmeter mode. 4 wire method eliminates resistance coming from probes. A 100 mA current was used for Ti composite samples and 1 A was used for copper sample. The resistance is automatically calculated by the source meter. In Table 9, the results of Ti composite samples are presented.

Table 9. Ti composite samples electrical resistance measurement results

Sample	Mean, Ω	Standard deviation, Ω	Sample size	Min, m Ω	Max, m Ω	Rotation, $^{\circ}$
N6	$5.84 \cdot 10^{-3}$	$8.06 \cdot 10^{-4}$	30	5.25795	9.89669	0
N6	$5.89 \cdot 10^{-3}$	$1.38 \cdot 10^{-3}$	30	5.46353	13.1977	45
N6	$3.20 \cdot 10^{-3}$	$8.42 \cdot 10^{-5}$	30	3.07321	3.39586	90
N6	$3.24 \cdot 10^{-3}$	$1.22 \cdot 10^{-4}$	30	3.02843	3.56487	135
N6	$3.20 \cdot 10^{-3}$	$1.00 \cdot 10^{-4}$	30	2.95689	3.33019	180
N6	$3.26 \cdot 10^{-3}$	$6.81 \cdot 10^{-5}$	30	3.15142	3.461616	225
N7	$4.89 \cdot 10^{-4}$	$5.23 \cdot 10^{-5}$	30	0.215748	0.515306	0
N7	$1.33 \cdot 10^{-3}$	$1.36 \cdot 10^{-4}$	30	0.618024	1.41909	45
N7	$5.09 \cdot 10^{-4}$	$2.01 \cdot 10^{-5}$	30	0.483832	0.604833	90
N7	$4.82 \cdot 10^{-4}$	$2.57 \cdot 10^{-5}$	30	0.461371	0.61004	135
N7	$9.18 \cdot 10^{-4}$	$8.08 \cdot 10^{-5}$	30	0.500315	0.972192	180
N7	$1.25 \cdot 10^{-3}$	$1.56 \cdot 10^{-4}$	30	0.43203	1.31425	225
N8	$1.38 \cdot 10^{-3}$	$1.16 \cdot 10^{-4}$	30	0.776787	1.45005	0
N8	$1.89 \cdot 10^{-3}$	$1.45 \cdot 10^{-4}$	30	1.15069	2.00726	45
N8	$1.05 \cdot 10^{-3}$	$1.26 \cdot 10^{-4}$	30	0.388065	1.10108	90
N8	$1.17 \cdot 10^{-3}$	$1.34 \cdot 10^{-4}$	30	0.47034	1.2293	135
N8	$6.15 \cdot 10^{-3}$	$5.60 \cdot 10^{-4}$	30	0.324264	0.654571	180
N8	$1.58 \cdot 10^{-3}$	$1.21 \cdot 10^{-4}$	30	0.95386	1.65238	225
N10	$1.43 \cdot 10^{-3}$	$1.86 \cdot 10^{-4}$	30	0.465897	1.51968	0
N10	$1.36 \cdot 10^{-3}$	$1.63 \cdot 10^{-4}$	30	0.506019	1.4278	45
N10	$1.44 \cdot 10^{-3}$	$1.78 \cdot 10^{-4}$	30	0.51074	1.53501	90
N10	$1.25 \cdot 10^{-3}$	$1.66 \cdot 10^{-4}$	30	0.374339	1.31324	135
N10	$1.67 \cdot 10^{-3}$	$1.61 \cdot 10^{-4}$	30	0.829292	1.76392	180
N10	$1.47 \cdot 10^{-3}$	$1.51 \cdot 10^{-4}$	30	0.687956	1.56081	225
G7	$1.32 \cdot 10^{-3}$	$1.76 \cdot 10^{-4}$	30	0.396438	1.40608	0
G7	$1.36 \cdot 10^{-3}$	$1.64 \cdot 10^{-4}$	30	0.49504	1.44038	45
G7	$1.25 \cdot 10^{-3}$	$1.56 \cdot 10^{-4}$	30	0.428495	1.34422	90
G7	$9.41 \cdot 10^{-3}$	$1.47 \cdot 10^{-4}$	30	0.169358	1.01955	135
G7	$1.36 \cdot 10^{-3}$	$1.74 \cdot 10^{-4}$	30	0.453201	1.43754	180
G7	$1.91 \cdot 10^{-3}$	$1.75 \cdot 10^{-4}$	30	0.995883	2.00025	225
G6	$1.77 \cdot 10^{-3}$	$1.58 \cdot 10^{-4}$	30	0.964574	1.89019	0
G6	$1.11 \cdot 10^{-3}$	$1.62 \cdot 10^{-4}$	30	0.262264	1.20556	45
G6	$1.36 \cdot 10^{-3}$	$2.13 \cdot 10^{-4}$	30	0.251124	1.45022	90
G6	$1.46 \cdot 10^{-3}$	$1.63 \cdot 10^{-4}$	30	0.60932	1.56586	135
G6	$1.43 \cdot 10^{-3}$	$1.45 \cdot 10^{-4}$	30	0.686721	1.53164	180
G6	$1.31 \cdot 10^{-3}$	$1.84 \cdot 10^{-4}$	30	0.351551	1.40101	225

Six Titanium composite samples were tested in total. One sample was measured six times, each time needle holder was rotated by 45 degrees. Additionally, at each position, 30 measurements are

performed by the meter. By using statistics function, mean, standard deviation, minimum and maximum values are calculated automatically by the meter. Furthermore, an average of the six measurements is calculated, the results are presented in Table 10. The Peltier element was used to maintain a constant 20 °C of the sample during measurement.

Table 10. Average electrical resistance measurement results

Sample	Mean, Ω	Standard deviation, Ω	Min, m Ω	Max, m Ω
N6	$4.11 \cdot 10^{-3}$	$4.28 \cdot 10^{-4}$	3.821905	6.141154
N7	$8.30 \cdot 10^{-4}$	$7.85 \cdot 10^{-5}$	0.451887	0.905952
N8	$1.28 \cdot 10^{-3}$	$1.16 \cdot 10^{-4}$	0.677334	1.349107
N10	$1.43 \cdot 10^{-3}$	$1.67 \cdot 10^{-4}$	0.562374	1.520077
G7	$1.36 \cdot 10^{-3}$	$1.65 \cdot 10^{-4}$	0.489736	1.441337
G6	$1.41 \cdot 10^{-3}$	$1.71 \cdot 10^{-4}$	0.520926	1.507413
Copper	$5.77 \cdot 10^{-6}$	$1.47 \cdot 10^{-6}$	0.004644	0.050341

Identical measurements are performed again, but with negative current. This is performed to offset thermoelectric voltage. This is called the current reversal method [27]. Thermoelectric voltage is offset by using the following equation:

$$U_M = \frac{U_{M+} - U_{M-}}{2} = \frac{(U_T + U^*) - (U_T - U^*)}{2} \quad (5)$$

where: U_M is the true voltage without thermoelectric voltage (V); U_{M+} is the voltage measured with positive current (V); U_{M-} is the voltage measured with negative current (V); U_T is the thermoelectric voltage (V); U^* is the true voltage without thermoelectric voltage (V).

The resistance values with offset thermoelectric voltage are presented in Table 11.

Table 11. Average electrical resistance measurement results after current reversal method

Sample	Mean, Ω	Standard deviation, Ω	Min, m Ω	Max, m Ω
N6	$2.50 \cdot 10^{-3}$	$3.28 \cdot 10^{-5}$	2.144444	3.67694233
N7	$7.02 \cdot 10^{-4}$	$5.20 \cdot 10^{-5}$	0.550093	0.84121925
N8	$1.21 \cdot 10^{-3}$	$7.87 \cdot 10^{-4}$	0.844191	1.27412183
N10	$1.34 \cdot 10^{-3}$	$1.03 \cdot 10^{-4}$	0.865272	1.42316083
G7	$1.29 \cdot 10^{-3}$	$1.05 \cdot 10^{-4}$	0.805087	1.38022808
G6	$1.33 \cdot 10^{-3}$	$1.04 \cdot 10^{-4}$	0.832173	1.40923183
Copper	$6.30 \cdot 10^{-6}$	$1.46 \cdot 10^{-6}$	0.004971	0.03053333

A copper sample is measured to test the accuracy and validity of the method and measurement. The copper sample was 10 mm in diameter and 6 mm in thickness. Resistivity is calculated by Eq. 2 and compared with the true resistivity of copper. A higher current of 1 A is used to measure the copper sample. The calculated electrical resistivity and electrical conductivity of all Ti composite samples, and copper sample is presented in Table 12. Electrical conductivity was calculated using Eq. 6.

$$\sigma = \frac{1}{\rho} \quad (6)$$

where: σ is the electrical conductivity of the sample material (S/m).

True resistivity of copper at 20 °C is $1.72 \cdot 10^{-8} \Omega\text{m}$. The measured and calculated copper resistivity was 4.6 times higher without correction factor and 3.3 times with correction factor applied. Such deviation could have come from the copper sample itself. It was not known if tested sample was pure copper. Also, the cleanliness of the sample and probes could have some influence. Furthermore, contact resistance of the probes to the sample brings error to the measurement. Sample was measured in regular air atmosphere and humidity.

Table 12. Samples electrical resistivity and conductivity

Sample	Electrical resistivity, Ωm	Electrical conductivity, S/m	Electrical resistivity with correction factor, Ωm	Electrical conductivity with correction factor, S/m
N6	$3.13 \cdot 10^{-5}$	$3.19 \cdot 10^4$	$2.27 \cdot 10^{-5}$	$4.40 \cdot 10^4$
N7	$8.82 \cdot 10^{-6}$	$1.13 \cdot 10^5$	$6.40 \cdot 10^{-6}$	$1.56 \cdot 10^5$
N8	$1.52 \cdot 10^{-5}$	$6.59 \cdot 10^4$	$1.10 \cdot 10^{-5}$	$9.09 \cdot 10^4$
N10	$1.68 \cdot 10^{-5}$	$5.94 \cdot 10^4$	$1.22 \cdot 10^{-5}$	$8.19 \cdot 10^4$
G7	$1.62 \cdot 10^{-5}$	$6.17 \cdot 10^4$	$1.18 \cdot 10^{-5}$	$8.51 \cdot 10^4$
G6	$1.67 \cdot 10^{-5}$	$5.99 \cdot 10^4$	$1.21 \cdot 10^{-5}$	$8.26 \cdot 10^4$
Copper	$7.91 \cdot 10^{-8}$	$1.26 \cdot 10^7$	$5.74 \cdot 10^{-8}$	$1.74 \cdot 10^7$

Another test was performed with different temperatures. Measurements were performed without rotating needle holder, only at one position. Measurements made for all six Ti composite samples and one copper sample. Peltier element used to heat and cool the sample. Firstly, measurements with cooling were performed. The negative and positive leads of the Peltier element was reversed. Sample was cooled until temperature reading was 10 °C. After measuring all the samples, Peltier element was used in heating mode to bring the sample temperature to 50 °C. An EX355P AIM-TTI programmable power supply was used to supply linear drive 12V and Peltier element needed current and voltage. The resistance measurement results are shown in Table 13.

Table 13. Samples resistance measurement results at different temperatures

Sample	Mean, Ω	Standard deviation, Ω	Sample size	Min, m Ω	Max, m Ω	Temperature, °C
N6	$2.09 \cdot 10^{-3}$	$1.12 \cdot 10^{-4}$	30	1.52524	2.15371	10
N7	$1.49 \cdot 10^{-3}$	$2.04 \cdot 10^{-4}$	30	0.416073	1.57574	10
N8	$1.87 \cdot 10^{-3}$	$1.33 \cdot 10^{-4}$	30	1.19103	1.9935	10
N10	$1.91 \cdot 10^{-3}$	$1.56 \cdot 10^{-4}$	30	1.12658	1.99966	10
G6	$1.31 \cdot 10^{-3}$	$1.47 \cdot 10^{-4}$	30	0.542653	1.3807	10
G7	$1.62 \cdot 10^{-3}$	$6.44 \cdot 10^{-5}$	30	1.327	1.71561	10
Copper	$1.74 \cdot 10^{-5}$	$1.08 \cdot 10^{-5}$	30	0.012896	0.074002	10
N6	$5.07 \cdot 10^{-4}$	$1.46 \cdot 10^{-5}$	30	0.486276	0.572001	50
N7	$1.04 \cdot 10^{-3}$	$9.18 \cdot 10^{-5}$	30	0.554988	1.0685	50
N8	$9.53 \cdot 10^{-4}$	$1.29 \cdot 10^{-4}$	30	0.277239	1.00512	50
N10	$1.10 \cdot 10^{-3}$	$1.38 \cdot 10^{-4}$	30	0.379099	1.17018	50
G6	$6.45 \cdot 10^{-4}$	$9.40 \cdot 10^{-5}$	30	0.377587	0.705361	50
G7	$1.12 \cdot 10^{-3}$	$1.26 \cdot 10^{-4}$	30	0.46116	1.18704	50
Copper	$4.57 \cdot 10^{-5}$	$2.03 \cdot 10^{-6}$	30	0.042646	0.543141	50

It was observed that all Ti composite samples had higher resistance at 10 °C than at 50 °C. Differently copper sample had lower resistance at 10 °C and higher at 50 °C. Typically resistance is lower at lower temperatures, but the composite samples act differently. A quite small temperature range is measured, other research shows linear increase of resistivity with increasing temperature, but measurements are made in higher temperatures [28]. A graph of electrical resistivity dependence on temperature is shown in Fig. 29.

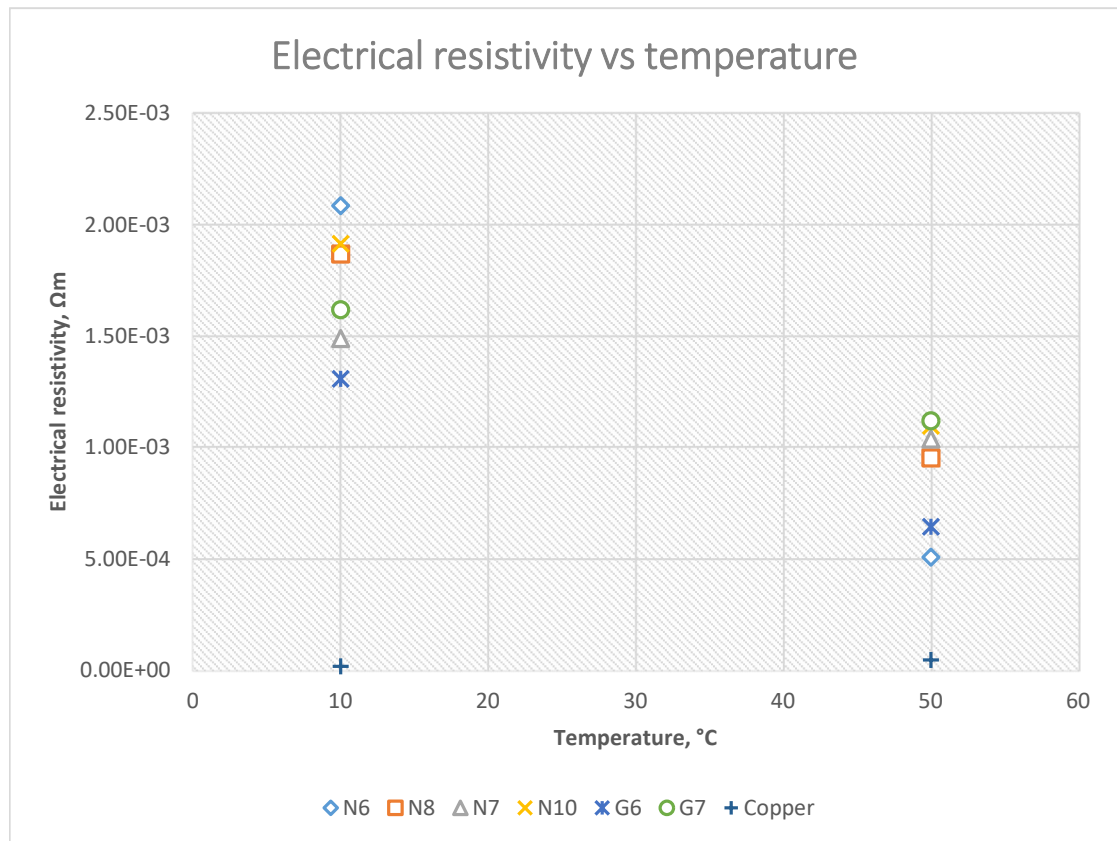


Fig. 29. Samples electrical resistivity dependence on temperature

The measurement procedure for measurements was:

1. Application of thermal paste to one side of sample.
2. Removing the needle holder and placing the sample with tweezers.
3. Pressing up button and lifting cylinder to top position so, that needles are contacting the sample. Since needles are spring loaded a constant 2 N force is applied.
4. Performing the measurement with Keithley 2614b source meter.
5. Lowering cylinder to bottom position by pressing down button.
6. Loosening needle holder fixation part.
7. Rotating needle holder 45 degrees if needed.
8. Repeating steps 3 – 7 until six measurements are made.
9. Removal of thermal paste from sample.

4.1. Discussion of measurement results

All measured composite samples had a composition of 75% Fe and 25% Ti. They were produced by mixing powders with HVED method. The current used and holding time for the HVED process was

different for each sample. After HVED process, samples were formed by using SPS method. The composition and fabrication parameters are shown in Table 14.

Table 14. Ti composite samples composition and fabrication parameters

Sample	Composition	HVED current, A	Holding time, min
N6	75% Fe – 25% Ti	1020	5
N7	75% Fe – 25% Ti	710	5
N8	75% Fe – 25% Ti	700	5
N10	75% Fe – 25% Ti	680	5
G6	75% Fe – 25% Ti	-	2
G7	75% Fe – 25% Ti	-	3

From the measurement results the N6 sample had the highest resistivity and the N7 had the lowest. Other samples had similar resistivity, around $1.2 \cdot 10^{-5} \Omega\text{m}$. The standard deviation was big compared to measured value; measurements had big variation. It appears that higher current results to bigger resistivity in the case of N6 sample. Holding time does not seem to influence the results. The experimental results were overall smaller than observed in similar research. All observed research tested Ti based composite samples, but the composition was different. Closest resistivity value was between Ti_3AlC_2 and N7 sample. A 1.2-time difference was observed between the two materials. The results obtained with simulation cannot be compared because a pure titanium material was used for sample. All Ti composites either tested by experimental method or found in literature had higher electrical resistivity than pure titanium. This can be explained by the microstructure of the composite. The microstructure has porosity and air gaps that increase the resistivity. Also, different particle material bonding could affect the overall resistivity. Furthermore, the alignment of the particles, whether isotropic or anisotropic affects result. The comparison of highest and lowest values obtained by different methods is presented in Table 15.

Table 15. Comparison of electrical resistivity obtained by different ways

Method	Highest electrical resistivity, Ωm	Lowest electrical resistivity, Ωm
Experimental	$2.27 \cdot 10^{-5}$	$6.4 \cdot 10^{-6}$
Found in similar research	$8.3 \cdot 10^{-6}$	$0.327 \cdot 10^{-6}$
Simulation of pure Ti sample	$3.46 \cdot 10^{-7}$	$3.46 \cdot 10^{-7}$

It was also observed that, tested composite samples had an unusual behavior, increase in resistivity while decreasing temperature. As seen in similar material research a linear increase in resistivity is seen at a certain range. However, nonlinear behavior can be exhibited at lower temperatures [29]. Measurements consisting of a wider range would be needed to determine if in fact this material behaves differently than other metals.

Measurement set up can be used not only for Ti composite materials, but also for other materials. Copper was measured and compared to the real value was in the order of 3 to 4 times. Increase of current is needed if higher electrical conductivity samples would be measured. Differently, lower current would be used for lower electrical conductivity samples would be used.

5. Cost analysis of fabricating electrical conductivity measurement setup

In this chapter, economical aspect of the measurement setup will be discussed. A cost analysis was performed for the electrical conductivity measurement setup. The cost of needed material for fabricating the measurement setup and performing measurements is presented in Table 16.

Table 16. Cost of material for electrical conductivity measurement setup

No.	Item	Cost, Eur
1	Polypropylene raw material 230 x 320 x 22 mm	80
2	Aluminum block 100 x 100 x 20 mm	70
3	Chromed cylinder rod 1 m	20
4	2 x aluminum cylinder rod 1 m	20
5	4 x test needles	20
6	Linear drive LA-T5 3500N 3mm/s 12V	84.7
7	Bolts and nuts	15
8	1 x Plastic bolt ISO 7045 - M3 x 30	3
9	4 x Bolt ISO 4762 M3 x 25	2
10	2 x Bolt ISO 4762 M6 x 35	2
11	11 x Bolt ISO 7380 - M5 x 12	5
12	2 x Bolt ISO 7045 - M3 x 10	1
13	2 x Nut ISO - 4034 - M6	1
14	4 x brackets	5
15	Washer D24	2
16	Peltier element 40 x 40 6A 24V	15
17	Arduino UNO module	10
18	ARDUINO 1602 2x16 LCD shield	7
19	3 x Silver thermal paste IPAS04AG	21
20	Teflon Wire CLA09012T 10m	5
21	Valve grinding paste	20
22	DS18B20 temperature sensor	8
23	Soldering wire	5
24	L298N motor driver	8
25	Cylindrical polypropylene raw material	20
26	2 x Copper sample	20
27	Keithley 2614B source meter	11800
28	EX355P AIM-TTI programmable power supply	470

Cost of raw material and parts was 469.7 Eur. This price doesn't include the needed devices for measurement such as a source meter or power supply, which is 12270 Eur. Also, all the equipment and tools needed to build the measurement setup is not considered. The labor time to build, design the equipment is shown in Table 17.

Table 17. Labor cost of fabricating measurement setup

Operation	Approximate time spent	Price, Eur
Turning	12	240
Milling	15	300
Drilling	20	400
Cutting	25	500
Grinding/polishing	10	150
Tapping	3	45
Soldering	3	45
Assembly	5	75
Modelling	20	300
Making drawings	15	225
Coding	5	75

For turning, milling, and drilling, cutting operations, 20 Eur per hour labor cost was used. This is a common labor price for metalwork. For other operations 15 Eur per hour labor cost was used. In total approximately 133 hours were needed to fabricate the measurement instrument. 40 hours were needed to perform 3D modelling, making drawings, and writing control program. The total cost for labor was 2355 Eur. The total cost of needed materials, tools and labor cost was 15094.74 Eur.

The biggest price influence comes from source meter. If source meter could be integrated with only the needed four wire measurement function, the price would drastically reduce. Also, if production would be optimized for serial production, the production price would be reduced. Cost of materials could be reduced if bought in large quantities from suppliers. Potentially, the total cost of the measurement setup could be reduced to 2000 – 3000 Eur.

Similar measurement setups in the market go for around 2000 Eur. Two main manufacturers of resistivity measurement devices can be found, Ossila Ltd and Jandel Engineering. Ossila is offering an all in one device with integrated source meter and software. The price is 1800 Eur [30]. An image of the Ossila measurement system is shown in Fig. 30.

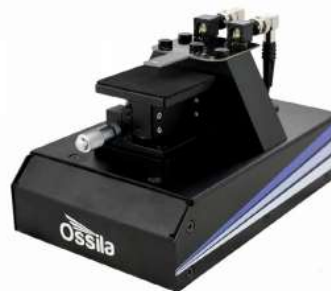


Fig. 30. Ossila Four-Point Probe System [30]

Most measurement systems found in the market are marketed for measuring thin semiconductor films. The proposed measurement setup is intended to be used for bulk samples. Metal or semiconductor samples could be used. The measurement setup could be improved by integrating source meter and making dedicated software or LCD screen that could show the final electrical conductivity value. Furthermore, other sample holders could be made for measurement of different geometry samples.

Conclusions

1. An electrical conductivity measurement setup was developed and tested. Titanium composite electrical conductivity successfully measured and calculated. Measurement setup operated as intended, none of the parts broke or deformed during measurements.
2. A design of the measurement setup was created using 3D modeling. The design conformed to needed requirements. Outer dimensions of the setup did not go over dimensions of the vacuum chamber. The outside dimensions of the measurement setup were 120 mm width, 228 mm length and 323 mm height. The samples fit into the sample holder and needles could probe them. The maximum sample diameter was 11 mm, and the minimum was 7 mm. The maximum sample thickness was 20 mm and minimum 4 mm. A heating and cooling element was applied. A minimum temperature of $-55\text{ }^{\circ}\text{C}$ and a maximum temperature of $83\text{ }^{\circ}\text{C}$ could be achieved. The sample can be measured at different angles by rotating needle holder. 9 drawings created for parts that will be fabricated. Simulation performed for the four-point probes with a pure titanium sample. Electrical resistivity calculated from simulation results was $3.46 \cdot 10^{-7}\ \Omega\text{m}$. The percentage error from true value was 10%.
3. It was possible to fabricate all parts with available tools. 18 parts were fabricated in total. 6 parts were bought, and 22 standard parts used. All parts could assemble and disassemble if needed. An Arduino module was programmed to control the linear drive and measure temperature.
4. Six Titanium composite samples electrical resistance measured. Electrical resistivity and conductivity calculated. N6 sample had the highest resistivity with $2.27 \cdot 10^{-5}\ \Omega\text{m}$ and the N7 had the lowest with $6.40 \cdot 10^{-6}\ \Omega\text{m}$. Other samples had similar resistivity, around $1.2 \cdot 10^{-5}\ \Omega\text{m}$. Additionally a copper sample was measured to validate the measurement. Result was $5.74 \cdot 10^{-8}\ \Omega\text{m}$, it was 3.3 times higher than the real value of copper. Additionally, all samples were measured at $10\text{ }^{\circ}\text{C}$ and $50\text{ }^{\circ}\text{C}$. It was observed that all Titanium composite samples had lower resistivity at $50\text{ }^{\circ}\text{C}$, but copper sample had lower resistivity at $10\text{ }^{\circ}\text{C}$. Experimental results were compared with similar research results. N7 sample and Ti_3AlC_2 had only 1.2 time difference. In all cases Titanium composite samples had lower electrical conductivity than pure Titanium.
5. A cost analysis was performed for the measurement setup. The total cost for the materials needed to fabricate the measurement setup was 469.7 Eur. The total cost for labor was 2355 Eur. Total cost including materials, labor and needed devices to complete measurements were 15094.74 Eur.

Recommendations for future research:

- Measurement of different composition and resistivity samples.
- Measurement of same Titanium composite samples at more different temperatures.
- Integrating software and source meter into measurement setup.
- Fabrication of universal sample holder to hold different geometry samples.
- Fabrication of needle holder with very accurate needle distances.
- Measurement in vacuum chamber for the elimination of outside influence.

List of references

1. HAYAT, Muhammad D., Harshpreet SINGH, Zhen HE and Peng CAO. Titanium metal matrix composites: An overview. *Composites Part A: Applied Science and Manufacturing* [online]. 2019, **121**, 418–438. ISSN 1359-835X. Available at: doi:10.1016/J.COMPOSITESA.2019.04.005
2. SYZONENKO, O M, S V PROKHORENKO, E V LYPYAN, A D ZAICHENKO, M S PRYSTASH, A S TORPAKOV, M O PASHCHYN, R VOINAROVSKA-NOVAK and E SHEREHII. PULSED DISCHARGE PREPARATION OF A MODIFIER OF Ti-TiC SYSTEM AND ITS INFLUENCE ON THE STRUCTURE AND PROPERTIES OF THE METAL. *Materials Science* [online]. 2020, **56**(2). Available at: doi:10.1007/s11003-020-00421-1
3. PRIKHNA, T. A., O. P. OSTASH, A. S. KUPRIN, V. Ya PODHURSKA, T. B. SERBENYUK, E. S. GEVORKYAN, M. RUCKI, W. ZUROWSKI, W. KUCHARCZYK, V. B. SVERDUN, M. V. KARPETS, S. S. PONOMARYOV, B. D. VASYLIV, V. E. MOSHCHIL and M. A. BORTNITSKAYA. A new MAX phases-based electroconductive coating for high-temperature oxidizing environment. *Composite Structures* [online]. 2021, **277**, 114649. ISSN 0263-8223. Available at: doi:10.1016/J.COMPSTRUCT.2021.114649
4. ZHOU, Weibing, Kang LI, Jiaoqun ZHU and Ruguang LI. In situ synthesis, mechanical and cyclic oxidation properties of Ti₃AlC₂/Al₂O₃ composites. *Advances in Applied Ceramics* [online]. 2018, **117**(6), 340–346. ISSN 1743-6761. Available at: doi:10.1080/17436753.2018.1434953
5. MOONA, Girija, R S WALIA, Vikas RASTOGI and Rina SHARMA. Aluminium metal matrix composites: A retrospective investigation. *Journal of Chemical Technology and Metallurgy* [online]. 2019, **54**(6), 1361–1370. ISSN 13147978. Available at: <https://core.ac.uk/download/pdf/229211628.pdf>
6. ZHOU, Dongshuai, Feng QIU, Huiyuan WANG and Qichuan JIANG. Manufacture of nano-sized particle-reinforced metal matrix composites: A review. *Acta Metallurgica Sinica (English Letters)* [online]. 2014, **27**(5), 798–805. ISSN 21941289. Available at: doi:10.1007/s40195-014-0154-z
7. MICCOLI, I., F. EDLER, H. PFNÜR and C. TEGENKAMP. The 100th anniversary of the four-point probe technique: The role of probe geometries in isotropic and anisotropic systems. *Journal of Physics Condensed Matter* [online]. 2015, **27**(22). ISSN 1361648X. Available at: doi:10.1088/0953-8984/27/22/223201
8. SINGH, N., P. HAMEED, R. UMMETHALA, G. MANIVASAGAM, K. G. PRASHANTH and J. ECKERT. Selective laser manufacturing of Ti-based alloys and composites: impact of process parameters, application trends, and future prospects. *Materials Today Advances* [online]. 2020, **8**, 100097. ISSN 2590-0498. Available at: doi:10.1016/J.MTADV.2020.100097
9. LIAQUAT, Hassan, Xiaoliang SHI, Kang YANG, Yuchun HUANG, Xiyao LIU and Zhihai WANG. Tribological Behavior of TiAl Metal Matrix Composite Brake Disk with TiC Reinforcement Under Dry Sliding Conditions. *Journal of Materials Engineering and Performance* [online]. no date, **26**. Available at: doi:10.1007/s11665-017-2789-1
10. FU, Zhezhen, Kanchan MONDAL and Rasit KOC. Sintering, mechanical, electrical and oxidation properties of ceramic intermetallic TiC-Ti₃Al composites obtained from nano-TiC particles. *Ceramics International* [online]. 2016, **42**(8), 9995–10005. ISSN 02728842. Available at: doi:10.1016/j.ceramint.2016.03.102
11. TORRES, Carlos, Roger QUISPE, Noely Z. CALDERÓN, Lara EGGERT, Marcus HOPFELD, Christopher ROJAS, Magali K. CAMARGO, Andreas BUND, Peter SCHAAF and Rolf GRIESELER. Development of the phase composition and the properties of Ti₂AlC and Ti₃AlC₂ MAX-phase thin films – A multilayer approach towards high phase purity. *Applied Surface Science* [online]. 2021, **537**, 147864. ISSN 0169-4332. Available at: doi:10.1016/J.APSUSC.2020.147864
12. TYRPEKL, V, C BERKMANN, M HOLZHÄUSER, F KÖPP, M COLOGNA, T WANGLE and

- J SOMERS. Implementation of a spark plasma sintering facility in a hermetic glovebox for compaction of toxic, radiotoxic, and air sensitive materials ARTICLES YOU MAY BE INTERESTED IN [online]. 2015. Available at: doi:10.1063/1.4913529
13. SHI, Shengfang, Sunghun CHO, Tomoyo GOTO and Tohru SEKINO. Fine Ti-dispersed Al₂O₃ composites and their mechanical and electrical properties [online]. 2018. Available at: doi:10.1111/jace.15472
 14. YE, Hui, Xiaoli CUI, Hongwei CUI, Xinghui LI, Ze ZHU, Yaokun PAN and Rui FENG. Study about improving mechanism of electrical conductivity of AA1070Al treated by a novel composite boron treatment with trace Ti. *Journal of Alloys and Compounds* [online]. 2021, **870**, 159416. ISSN 0925-8388. Available at: doi:10.1016/J.JALLCOM.2021.159416
 15. WANG, Zhenwei and Yating YU. Traditional Eddy Current-Pulsed Eddy Current Fusion Diagnostic Technique for Multiple Micro-Cracks in Metals [online]. 2018. Available at: doi:10.3390/s18092909
 16. ASMATULU, R, P K BOLLAVARAM, V R PATLOLLA, I M ALARIFI and W S KHAN. Investigating the effects of metallic submicron and nanofilms on fiber-reinforced composites for lightning strike protection and EMI shielding [online]. no date. Available at: doi:10.1007/s42114-020-00135-7
 17. ALEMOUR, Belal, Omar BADRAN and Mohd Roshdi HASSAN. A Review of Using Conductive Composite Materials in Solving Lightning Strike and Ice Accumulation Problems in Aviation. *Journal of Aerospace Technology and Management* [online]. 2019, **11**, 1–23. ISSN 2175-9146. Available at: doi:10.5028/jatm.v11.1022
 18. PANDEY, Shivendra Kumar and Anbarasu MANIVANNAN. A fully automated temperature-dependent resistance measurement setup using van der Pauw method. *Review of Scientific Instruments* [online]. 2018, **89**(3). ISSN 10897623. Available at: doi:10.1063/1.4998340
 19. BISHARA, Hanna, Matteo GHIDELLI and Gerhard DEHM. Approaches to Measure the Resistivity of Grain Boundaries in Metals with High Sensitivity and Spatial Resolution: A Case Study Employing Cu. *ACS Applied Electronic Materials* [online]. 2020, **2**(7), 2049–2056. ISSN 26376113. Available at: doi:10.1021/acsaelm.0c00311
 20. PENG, L. M. Preparation and properties of ternary Ti₃AlC₂ and its composites from Ti-Al-C powder mixtures with ceramic particulates. *Journal of the American Ceramic Society* [online]. 2007, **90**(4), 1312–1314. ISSN 00027820. Available at: doi:10.1111/j.1551-2916.2007.01517.x
 21. PARK, Menlo. Collinear four-point probe head and mount for resistivity measurements. US4267506A. 1981.
 22. CORPORATION, Plenum Publishing, Industrial LABO and Assistant Examiner-diep DO. Apparatus for measuring the surface resistance and electrical resistivity of a homogeneous resistive material at high temperature. US5656940A. 1997.
 23. SINGH, Saurabh and Sudhir K. PANDEY. Fabrication of Simple Apparatus for Resistivity Measurement in High-Temperature Range 300-620 K. *IEEE Transactions on Instrumentation and Measurement* [online]. 2018, **67**(9), 2169–2176. ISSN 00189456. Available at: doi:10.1109/TIM.2018.2811282
 24. SCHRODER DIETER K. *MATERIAL AND DEVICE SEMICONDUCTOR MATERIAL AND DEVICE Third Edition*. 2006. ISBN 9780471739067.
 25. NICA, Simona Luminita, Camelia HULUBEI, Iuliana STOICA, Emil Ghiocel IOANID, Valentin NICA and Silvia IOAN. Electrical resistivity under different humidity conditions for plasma-treated and gold-sputtered polyimide films. *Polymer Bulletin* [online]. 2016, **73**(6), 1531–1544. ISSN 01700839. Available at: doi:10.1007/S00289-015-1560-8
 26. TOPSOE, Haldor. *Geometric factors in four point resistivity measurement*. 2nd revise. 1968.
 27. KEITHLEY. Low Level Measurements Handbook. *Book* [online]. 2016, vi, I–5. Available at: <http://goo.gl/dGoppA>
 28. WANG, Ping, Bing chu MEI, Xiao lin HONG and Wei bing ZHOU. Synthesis of Ti₂AlC by hot pressing and its mechanical and electrical properties. *Transactions of Nonferrous Metals Society of China (English Edition)* [online]. 2007, **17**(5), 1001–1004. ISSN 10036326. Available

- at: doi:10.1016/S1003-6326(07)60215-5
29. HALIM, Joseph, Ingemar PERSSON, Eun Ju MOON, Philipp KÜHNE, Vanya DARAKCHIEVA, Per O.Å. PERSSON, Per EKLUND, Johanna ROSEN and Michel W. BARSOUM. Electronic and optical characterization of 2D Ti₂C and Nb₂C (MXene) thin films. *Journal of Physics Condensed Matter* [online]. 2019, **31**(16). ISSN 1361648X. Available at: doi:10.1088/1361-648X/ab00a2
30. OSSILA. *Four-Point Probe* [online] [viewed 2022-05-19]. Available at: <https://www.ossila.com/products/four-point-probe-system?variant=31916571009>

Appendices

Appendix 1. Arduino control program

```
#include <LiquidCrystal.h>
#include <OneWire.h>
#include <DallasTemperature.h>

#define ENA_PIN 3 // the Arduino pin connected to the EN1 pin L298N
#define IN1_PIN 11 // the Arduino pin connected to the IN1 pin L298N
#define IN2_PIN 12 // the Arduino pin connected to the IN2 pin L298N
#define POTENTIOMETER_PIN A1 // the Arduino pin connected to the potentiometer of the
actuator

#define ONE_WIRE_BUS 2

int lcdkeys;

#define STROKE_LENGTH 50 // PLEASE UPDATE THIS VALUE (in millimeter)
#define POTENTIOMETER_MAX 886 // PLEASE UPDATE THIS VALUE
#define POTENTIOMETER_MIN 137 // PLEASE UPDATE THIS VALUE
OneWire oneWire(ONE_WIRE_BUS);
DallasTemperature sensors(&oneWire);
LiquidCrystal lcd(8, 9, 4, 5, 6, 7); // Arduino lcd sheild pins defined

int targetPosition_mm = 13;

void setup() {
  Serial.begin(9600);
  pinMode(ENA_PIN, OUTPUT);
  pinMode(IN1_PIN, OUTPUT);
  pinMode(IN2_PIN, OUTPUT);

  digitalWrite(ENA_PIN, HIGH);

  lcd.begin(16, 2);
  sensors.begin();
}

void loop() {

  int potentiometer_value = analogRead(POTENTIOMETER_PIN);
  int stroke_pos = map(potentiometer_value, POTENTIOMETER_MIN,
POTENTIOMETER_MAX, 0, STROKE_LENGTH);
  Serial.print("The stroke's position = ");
```

```

Serial.print(stroke_pos);
Serial.println(" mm");

Serial.print(" Requesting temperatures...");
sensors.requestTemperatures(); // Send the command to get temperature readings
Serial.println("DONE");
/*****/
Serial.print("Temperature is: ");
Serial.print(sensors.getTempCByIndex(0)); // Why "byIndex"?
  delay(1000);

  lcd.setCursor(0, 0);
  lcd.print("Temp in C:");
  lcd.setCursor(11, 0);
  lcd.print(sensors.getTempCByIndex(0));

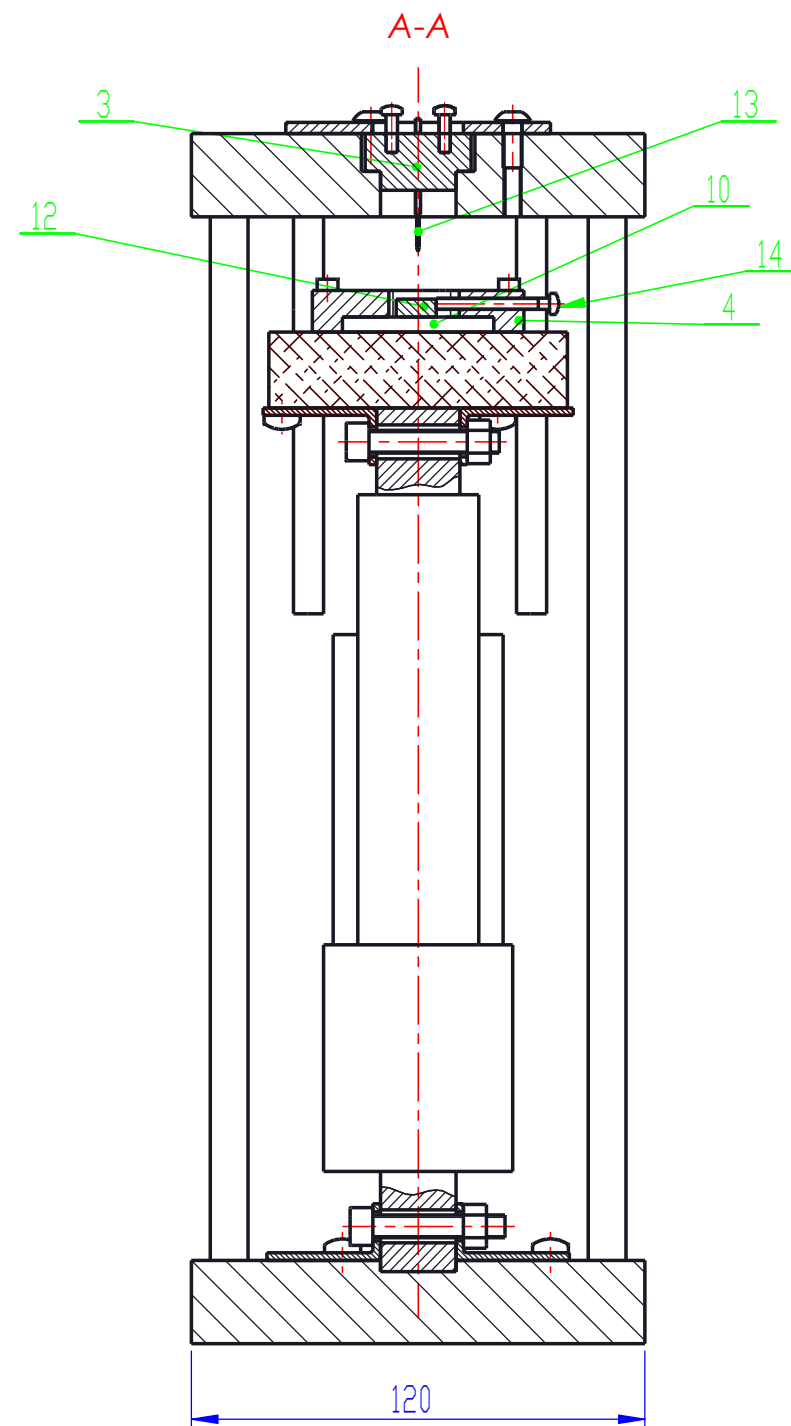
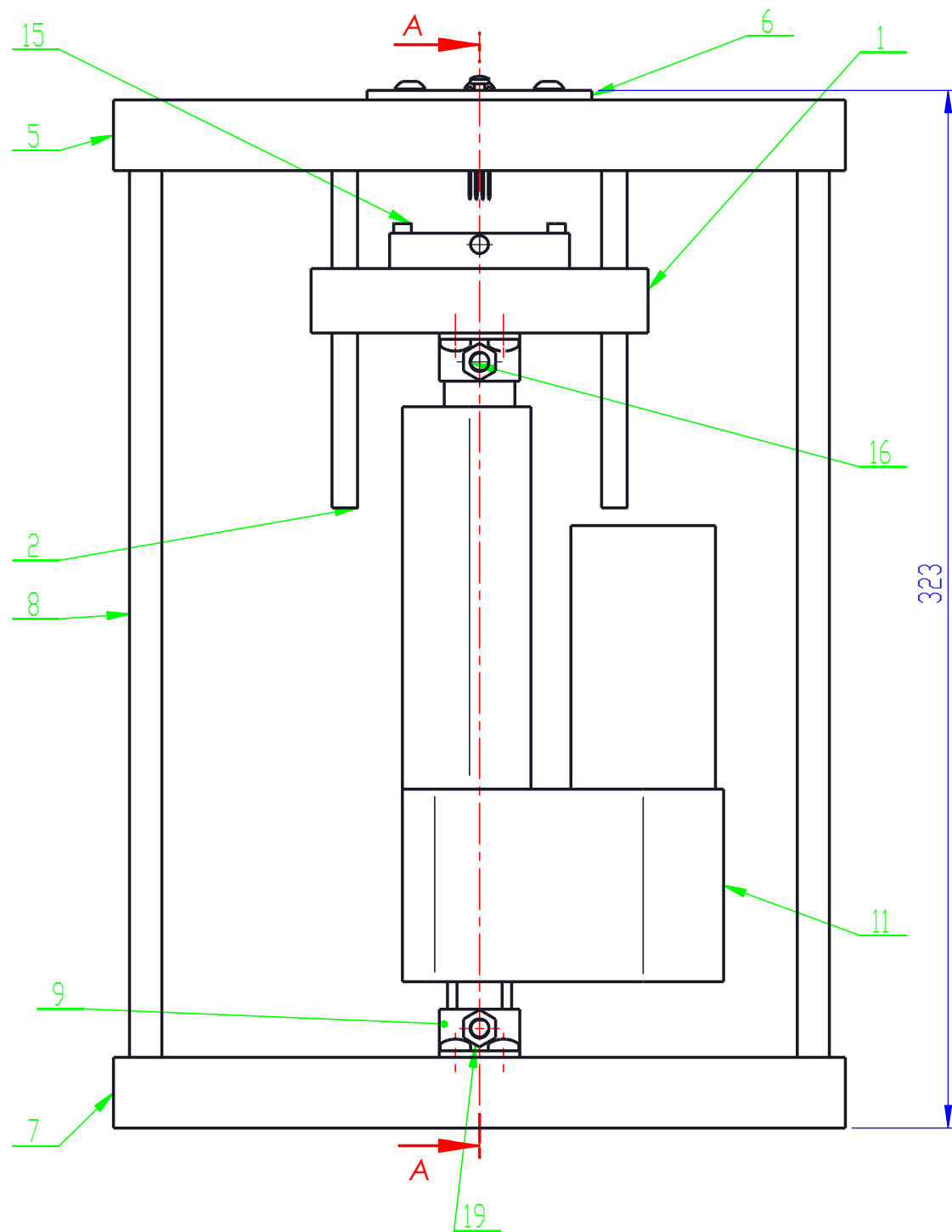
  delay(200);

Serial.println(lcdkeys);
  lcdkeys=analogRead(0);
  if(lcdkeys<50) {
  ACTUATOR_stop();
  }
  else if (lcdkeys<195) {
  ACTUATOR_extend();
  }
  else if(lcdkeys<380) {
  ACTUATOR_retract();
  }
  if (digitalRead(IN1_PIN)==HIGH & stroke_pos > targetPosition_mm)
  ACTUATOR_stop();

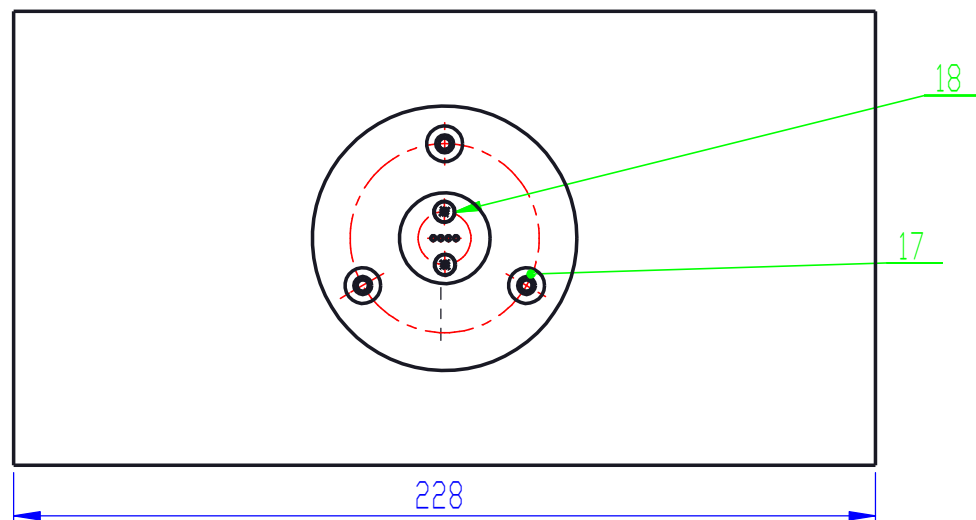
  }
void ACTUATOR_extend() {
  digitalWrite(IN1_PIN, HIGH);
  digitalWrite(IN2_PIN, LOW);
  }
void ACTUATOR_retract() {
  digitalWrite(IN1_PIN, LOW);
  digitalWrite(IN2_PIN, HIGH);
  }

void ACTUATOR_stop() {
  digitalWrite(IN1_PIN, LOW);
  digitalWrite(IN2_PIN, LOW);
  }

```

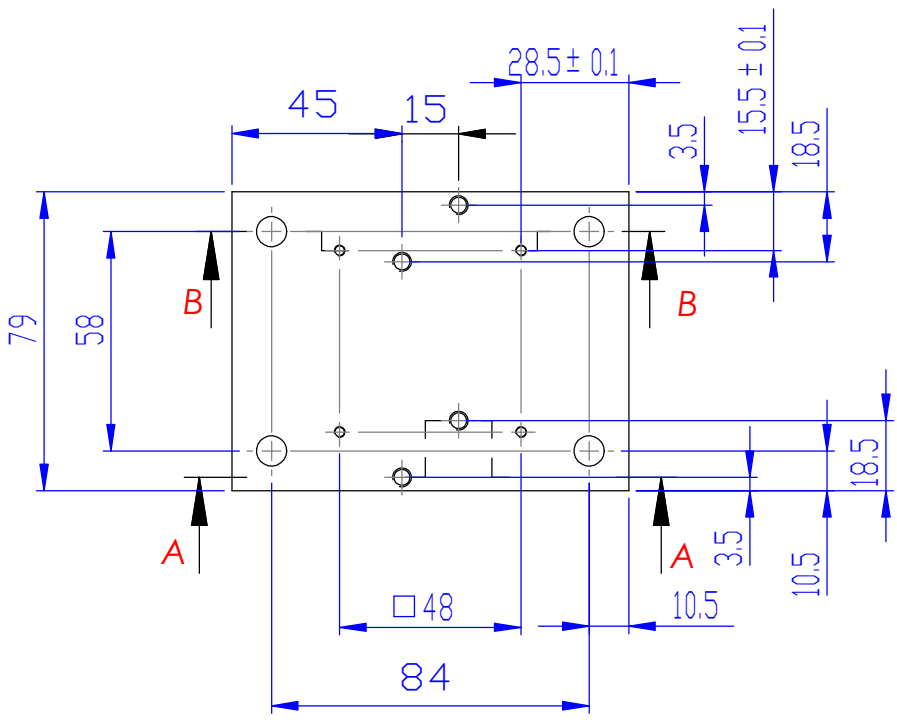
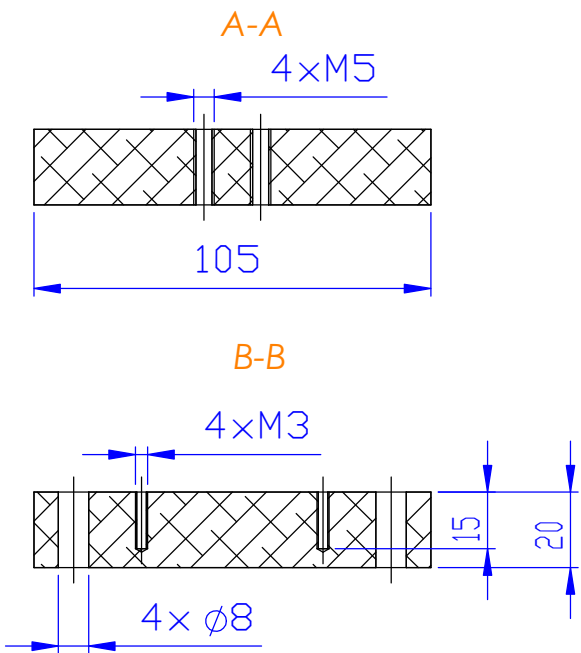


ITEM No.	PART	DRAWING No.	QTY.
1	Cooling element	TK.DG.01.00.01	1
2	Linear guide	TK.DG.01.00.02	4
3	Needle holder	TK.DG.01.00.03	1
4	Sample holder	TK.DG.01.00.04	1
5	Top housing	TK.DG.01.00.05	1
6	Fixing element	TK.DG.01.00.06	1
7	Bottom housing	TK.DG.01.00.07	1
8	Housing rod	TK.DG.01.00.08	4
9	Bracket	TK.DG.01.00.09	4
10	Peltier element 40 x 40		1
11	Linear actuator LA T5 3500N		1
12	Pellet		1
13	Needle		4
14	Bolt ISO 7045 - M3 x 30 - Z - 25N		1
15	Bolt ISO 4762 M3 x 25 - 18N		4
16	Bolt ISO 4762 M6 x 35 - 24N		2
17	Bolt ISO 7380 - M5 x 12 - 12N		11
18	Bolt ISO 7045 - M3 x 10 - Z - 10N		2
19	Nut ISO - 4034 - M6 - N		2



General tolerances as per LST EN 22768-mK

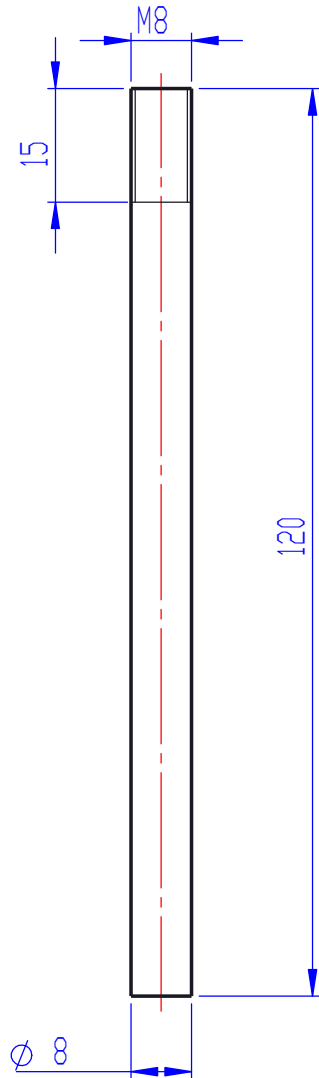
	File name	Additional information	Material	Scale 1:2
	Resp. department MED	Technical reference	Document type Assembly drawing	Document status
	Legal owner ktu kaunas university of technology 1922	Created by Donatas Gričius Approved by Rasa Kandrotaitė Janutiene	Title, Supplementary title Electrical conductivity measurement setup	TK.DG.01.00.00 AD
	Rev. A	Date 2022-05-09	Lang. En	Sheet 1/1



1. Unspecified tolerance limit according LST EN 22768-mK.
2. Unspecified radius of fillets R=0.5 mm.

√ Ra 6.3 (✓)

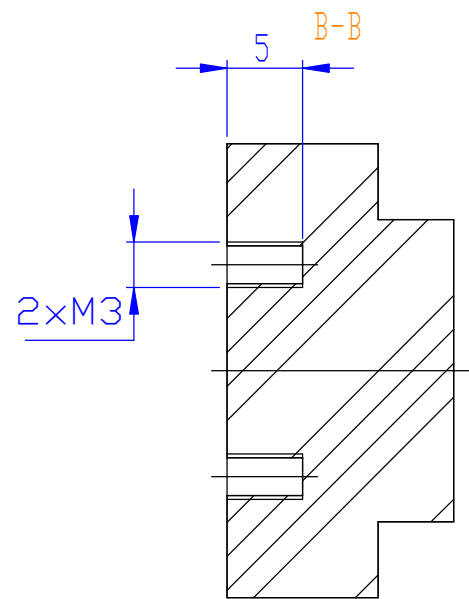
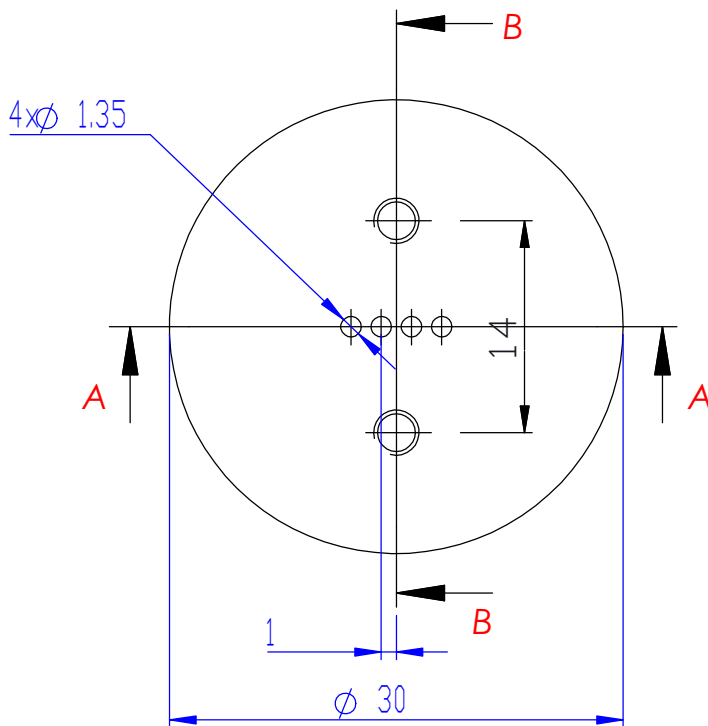
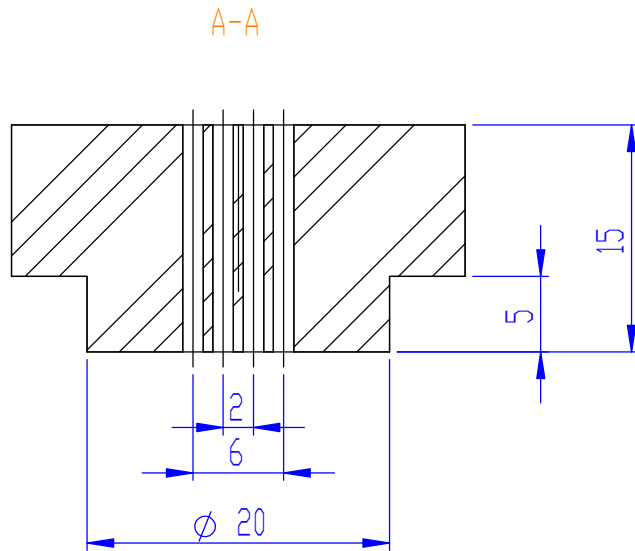
	File name	Additional information	Material Aluminium	Scale 1:2
Resp. department MIDF	Technical reference	Dokumento tipas Part drawing		Document status
Legal owner 	Created by Donatas Gričius	Title, Supplementary title Cooling element		TK.DG.01.00.01
	Approved by Rasa Kandrotaitė Janutiene'	Rev. A	Date 2022-05-09	Lang. En Sheet 1/1



1. Unspecified tolerance limit according LST EN 22768-mk.
2. Unspecified radius of fillets R=0.5 mm.

√ Ra 6.3 (✓)

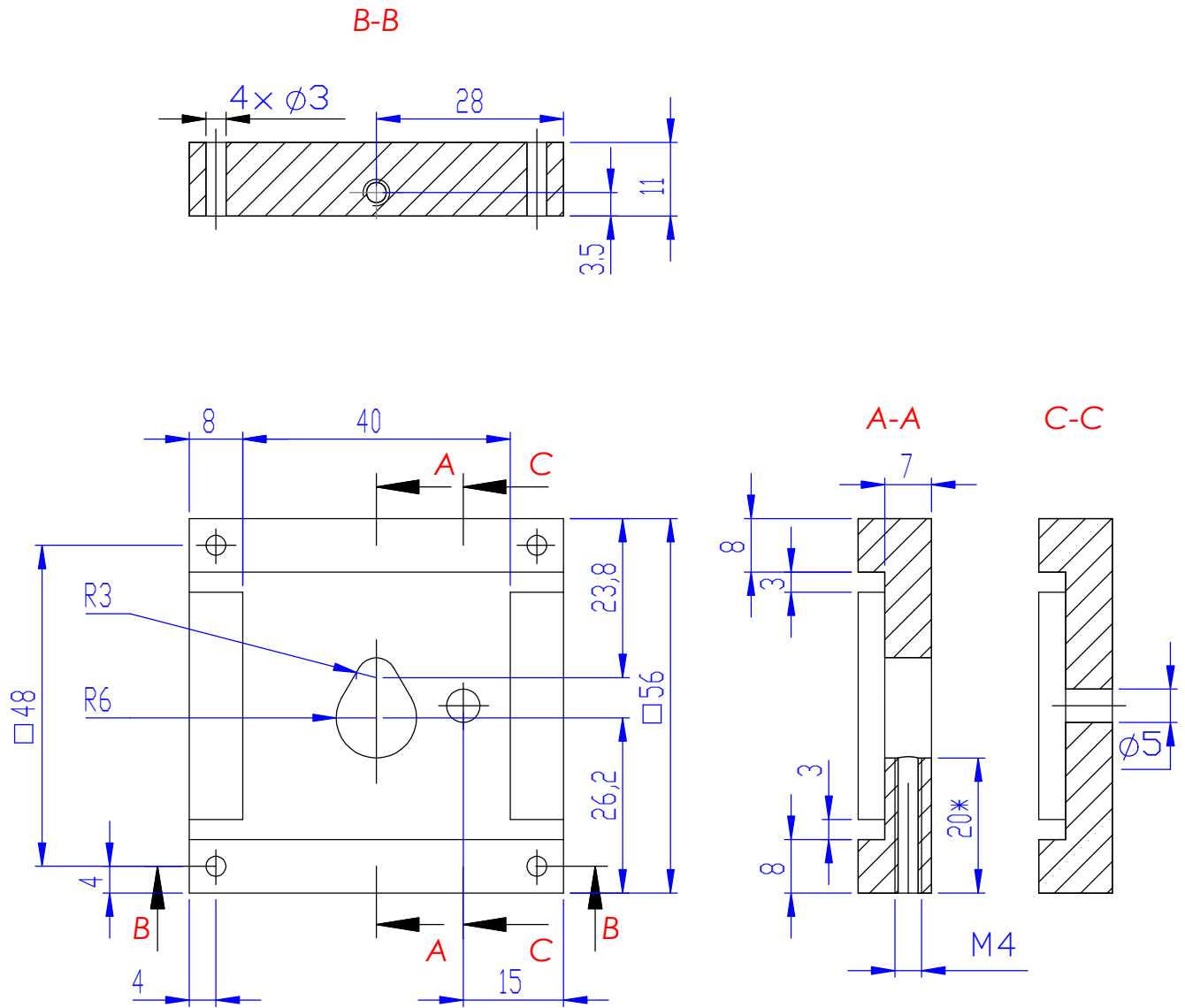
	File name	Additional information	Material Chromed steel	Scale 1:1
Resp. department MIDF	Technical reference	Dokumento tipas Part drawing		Document status
Legal owner 	Created by Donatas Gričius	Title, Supplementary title Linear Guide		TK.DG.01.00.02
	Approved by	Rev. A	Date 2022-05-09	Lang. En Sheet 1/1



1. Unspecified tolerance limit according LST EN 22768-mK.
2. Unspecified radius of fillets R=0.5 mm.

$\sqrt{Ra\ 6.3}$ (✓)

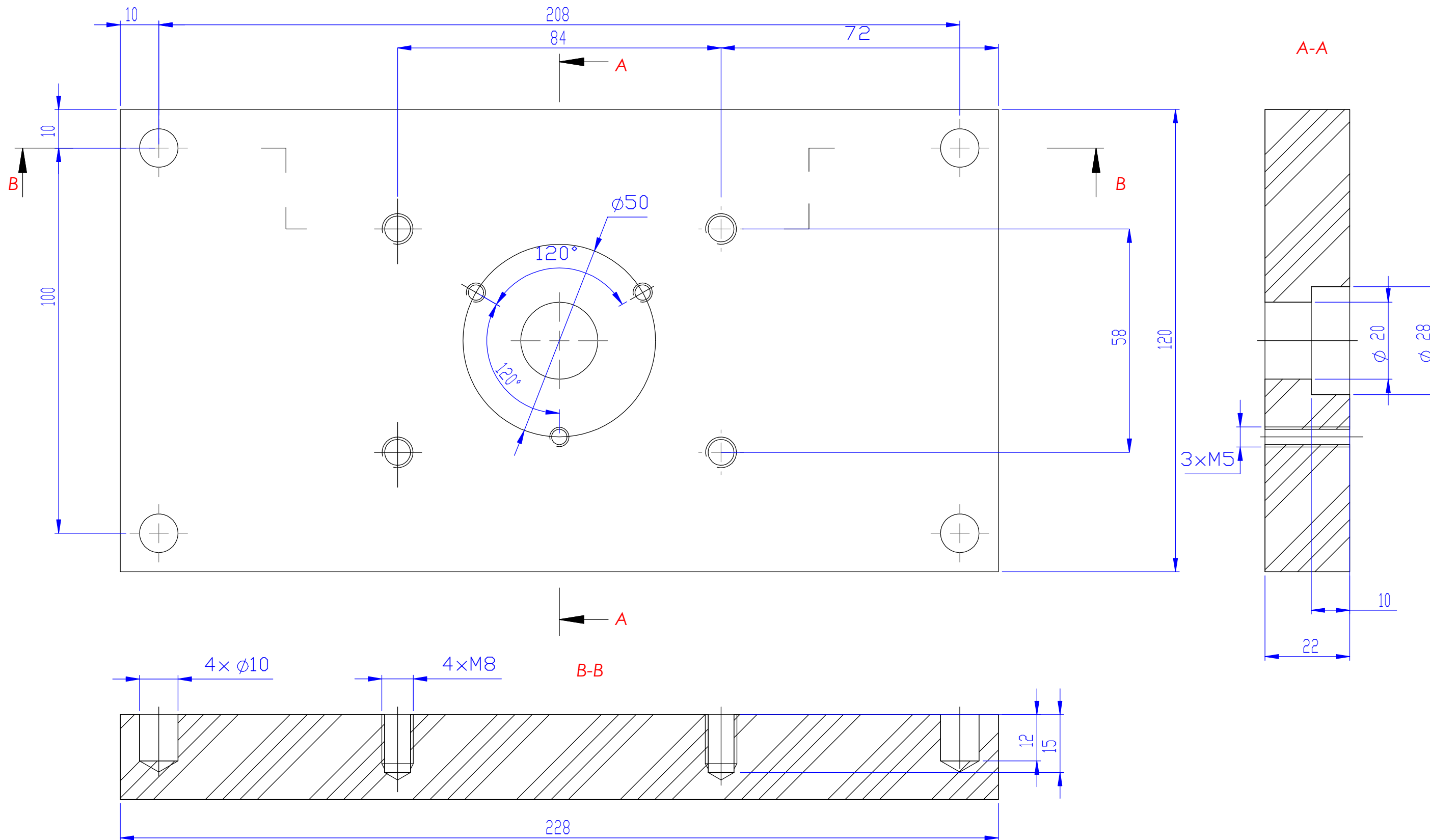
	File name	Additional information	Material Polypropylene	Scale 2:1
Resp. department MIDF	Technical reference	Dokumento tipas Part drawing	Document status	
Legal owner 	Created by Donatas Gričius	Title, Supplementary title Needle holder	TK.DG.01.00.03	
	Approved by Rasa Kandrotaitė Janutienė		Rev. A	Date 2022-05-09
			Lang. En	Sheet 1/1



1. Unspecified tolerance limit according LST EN 22768-mk.
2. Unspecified radius of fillets R=0.5 mm.
3. * - informational dimension.

√ Ra 6.3 (✓)

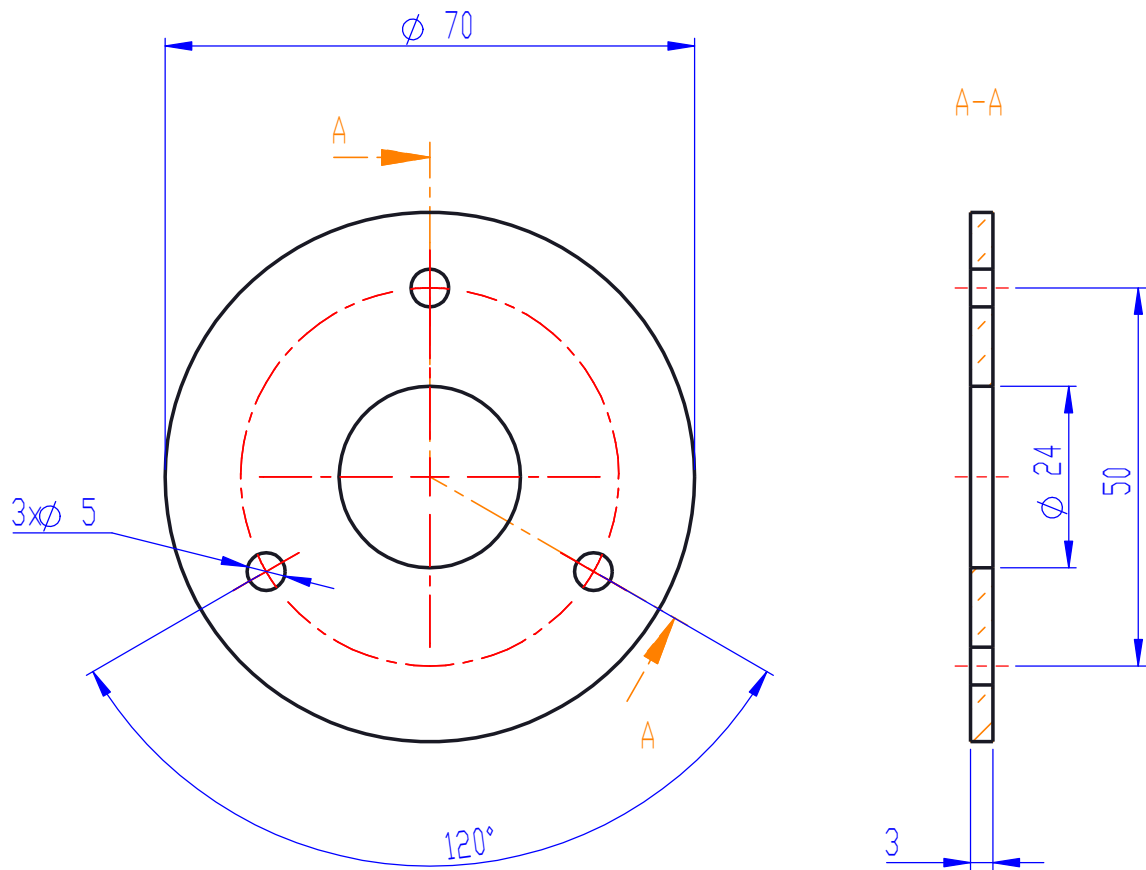
	File name	Additional information	Material Polypropylene	Scale 1:1	
Resp. department MIDF	Technical reference	Dokumento tipas Part drawing		Document status	
Legal owner	Created by Donatas Gričius	Title, Supplementary title Sample holder		TK.DG.01.00.04	
	Approved by Rasa Kandrotaitė Janutienė				Rev. A



General tolerances as per LST EN 22768-mK

$\sqrt{Ra\ 6,3}$ (✓)

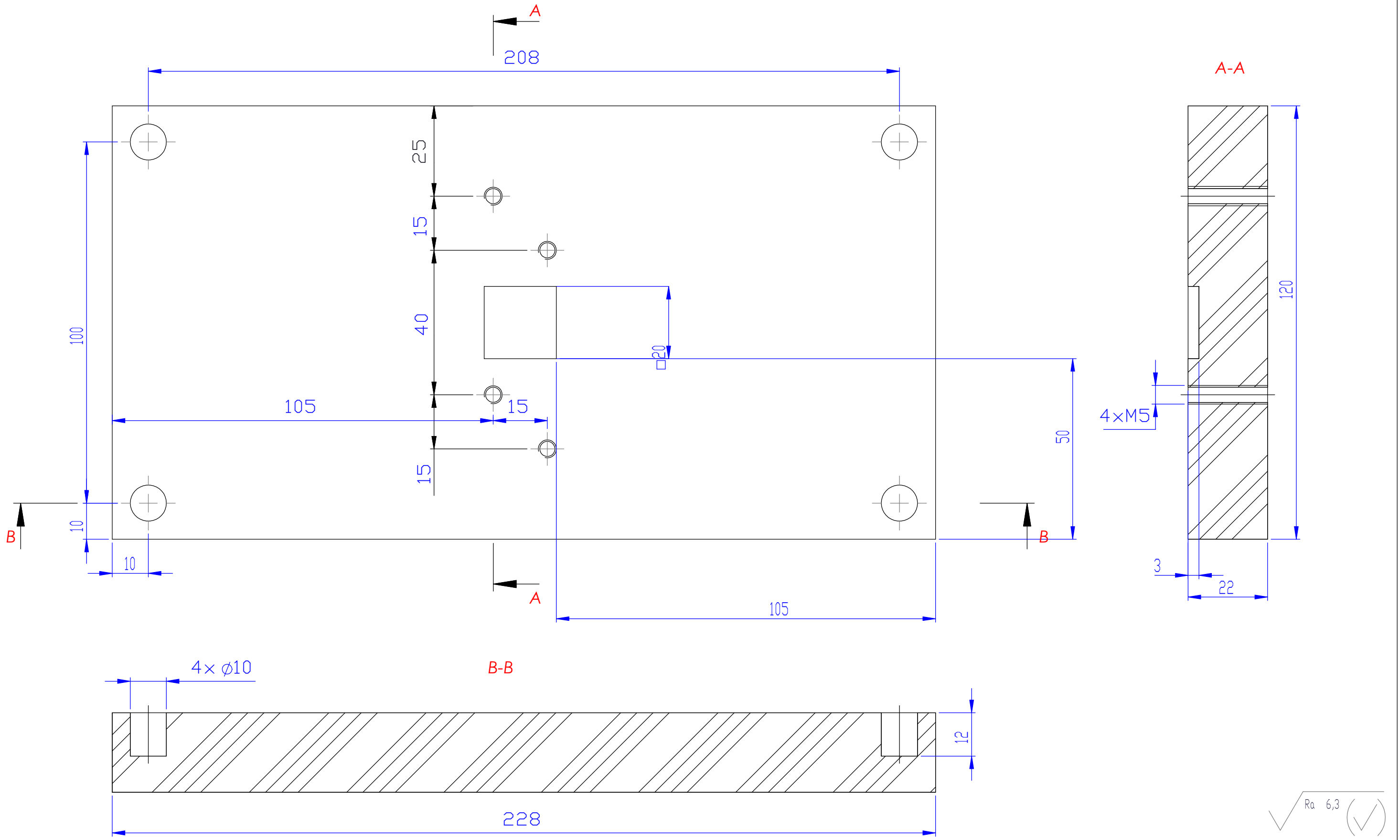
	File name	Additional information	Material Polypropylene	Scale 1:1
Resp. department MED	Technical reference	Document type Part drawing	Document status	
Legal owner 	Created by Donatas Gričius	Title, Supplementary title Top Housing	TK.DG.01.00.05	
	Approved by Rasa Kandrotaitė Janutiene		Rev. A	Date 2022-05-09
			Lang. En	Sheet 1/1



1. Unspecified tolerance limit according LST EN 22768-mk.
2. Unspecified radius of fillets $R=0.5$ mm.

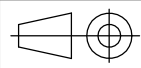

$\sqrt{Ra 6.3}$ (✓)

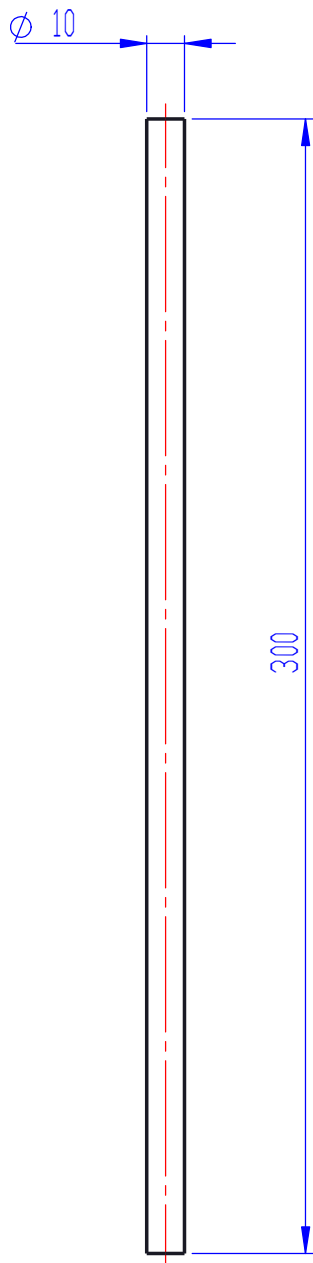
	File name	Additional information	Material Steel	Scale 1:1
Resp. department MIDF	Technical reference	Dokumento tipas Part drawing	Document status	
Legal owner 	Created by Donatas Gričius	Title, Supplementary title Fixing element	TK.DG.01.00.06	
	Approved by		Rev. A	Date 2022-05-09
			Lang. En	Sheet 1/1



General tolerances as per LST EN 22768-mK

√ Ra 6,3 (✓)

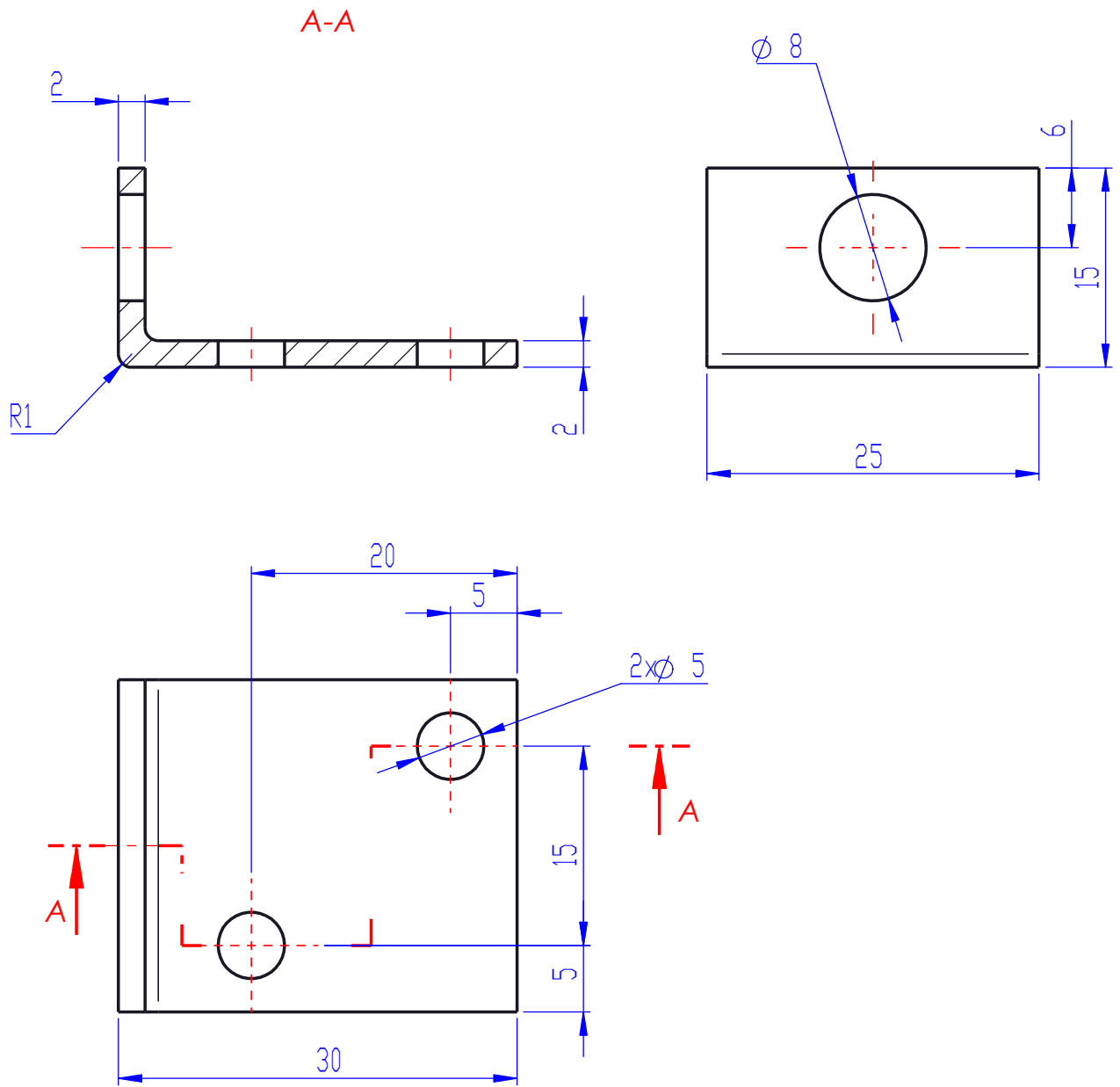
		File name	Additional information	Material Polypropylene	Scale 1:1
Resp. department MED	Technical reference	Document type Part drawing		Document status	
Legal owner  kaunas university of technology	Created by Donatas Gričius	Title, Supplementary title Bottom Housing		TK.DG.01.00.07	
	Approved by Rasa Kandrotaitė Janutiene	Rev. A	Date 2022-05-09	Lang. En	Sheet 1/1



1. Unspecified tolerance limit according LST EN 22768-mK.
2. Unspecified radius of fillets $R=0.5$ mm.



	File name	Additional information	Material Aluminium	Scale 1:2
Resp. department MIDF	Technical reference	Dokumento tipas Part drawing	Document status	
Legal owner 	Created by Donatas Gričius	Title, Supplementary title Housing rod	TK.DG.01.00.08	
	Approved by Rasa Kandrotaitė Janutienė		Rev. A	Date 2022-05-09
			Lang. En	Sheet 1/1



1. Unspecified tolerance limit according LST EN 22768-mK.
2. Unspecified radius of fillets R=0.5 mm.

$\sqrt{\text{Ra } 6.3}$ (✓)

	File name	Additional information	Material Steel	Scale 2:1
Resp. department MIDF	Technical reference	Dokumento tipas Part drawing		Document status
Legal owner Kauno technologijos universitetas	Created by Donatas Gričius	Title, Supplementary title Bracket		TK.DG.01.00.09
	Approved by	Rev. A	Date 2022-05-09	Lang. En Sheet 1/1